Networks and Heterogeneous Media

https://www.aimspress.com/journal/nhm

NHM, 21(4): 1450–1478.
DOI: 10.3934/nhm.2026055
Received: 21 April 2026
Revised: 15 June 2026
Accepted: 17 June 2026
Published: 06 July 2026

Research article

Threshold dynamics of a Reaction–Diffusion SIS Model with logistic growth and boundary outflow

Yifei Pan[1], **Heejung Byun**[1,*] **and Feng Li**[2]

[1] Department of Information Communication Technology, The University of Suwon, Hwaseong 18323, South Korea

[2] School of Mathematics and Statistic, Linyi University, Linyi 276005, China

* **Correspondence:** Email: heejungbyun@suwon.ac.kr; Tel: +82312298048; Fax: +82312298281.

Abstract: This study presents a reaction-diffusion framework that integrates boundary outflow mechanisms with logistic population dynamics to investigate epidemic evolution in spatially non-uniform environments. By incorporating non-linear, density-dependent regulation and boundary leakage, the model builds on the constraints of population conservation or closed habitats found in classical studies, thus offering a more objective representation of open population dynamics under resource limitations. We provide a rigorous analysis of the system's foundational mathematical properties, establishing the invariant non-negativity of state variables and uniform upper bounds for all global solutions, thereby ensuring the reliability of the subsequent dynamical analysis. Based on the spectral radius characterizations, the fundamental parameter $\mathcal{R}_0$ acts as the definitive threshold for disease control: the infection is destined for extinction when $\mathcal{R}_0 < 1$, whereas the system exhibits spatial persistence and the emergence of at least one non-trivial endemic equilibrium when $\mathcal{R}_0 > 1$. The findings reveal that the boundary outflow mechanism remains an effective mitigation strategy in resource-constrained environments, thereby significantly mitigating the infection pressure and suppressing the spatial dissemination of the disease.

Keywords: SIS epidemic model; logistic growth; boundary outflow; Principal eigenvalue; threshold dynamics

1. Introduction

The non-uniformity of the habitat and the way individuals move within it exerts a profound influence on the transmission process of infectious diseases. Accordingly, reaction–diffusion epidemic models are widely used to capture disease evolution driven by local transmission and spatial dispersal. Among them, SIS-type models have received extensive attention due to their applicability to diseases, where

individuals do not acquire long-term immunity after infection. In many classic spatial SIS models, a notable feature is that the total population remains preserved during the evolution process. This conservation mainly stems from two aspects: first, the model does not consider population change mechanisms such as birth and natural death; and second, the imposed homogeneous Neumann boundary conditions effectively prevent the migration of individuals at the boundaries. Under this setting, the long-time evolution is typically resolved by analyzing the stability of the infection-free steady state. By calculating the threshold R_0 through linearization at the disease-free equilibrium point, definitive threshold dynamics have been established in various scenarios.

Against this background, Allen et al. [1] formulated a pioneering spatially heterogeneous SIS reaction–diffusion model to investigate how spatial movement and local disease transmission together affect epidemic dynamics. Their model is given by the following:

$$\begin{cases} S_t = d_S \Delta S - \beta(x)\dfrac{SI}{S+I} + \gamma(x)I, & x \in \Omega,\ t > 0, \\ I_t = d_I \Delta I + \beta(x)\dfrac{SI}{S+I} - \gamma(x)I, & x \in \Omega,\ t > 0, \\ \dfrac{\partial S}{\partial n} = \dfrac{\partial I}{\partial n} = 0, & x \in \partial\Omega,\ t > 0, \\ S(x,0) = S_0(x) \geq 0, \quad I(x,0) = I_0(x) \geq 0,\ I_0 \not\equiv 0, & x \in \Omega. \end{cases} \tag{1.1}$$

In this model, $S(x,t)$ and $I(x,t)$ represent the spatial densities of susceptible and infected individuals, respectively, for $x \in \Omega$ and $t > 0$. Both populations diffuse in space with constant diffusion coefficients d_S and d_I. Spatial heterogeneity in disease transmission and recovery is incorporated through the functions $\beta(x)$ and $\gamma(x)$, which are taken to be positive and Hölder continuous on Ω. We assume Ω is a bounded region in $\mathbb{R}^m$ with a C^2 boundary $\partial\Omega$, and let $\partial/\partial n$ be the outward normal derivative operator on the boundary. For the initial conditions, the functions $S_0(x)$ and $I_0(x)$ are assumed to be positive on Ω, with $I_0 \not\equiv 0$, thus ensuring that the system starts from a biologically meaningful configuration containing a nontrivial amount of infection.

By defining the basic reproduction number $\mathcal{R}_0$, Allen et al. [1] established a fundamental threshold framework for epidemic dynamics. Their findings indicate that infection is globally eradicated when $\mathcal{R}_0 < 1$, as the disease-free state remains the unique attractor. Conversely, for $\mathcal{R}_0 > 1$, this steady state becomes unstable, giving rise to a persistent endemic equilibrium. Beyond identifying this transition, the study delved into the spatial profiles of the infectious population. Their analysis revealed that a larger diffusion of the infected population facilitates spatial spread and persistence across the entire domain, while a smaller diffusion may cause the infection to localize in high-risk regions. Building on the foundational SIS model of Allen et al. [1], numerous extensions have been developed under the assumption of population conservation. These extensions include models with temporal periodicity [2–4], models that incorporate delay effects [5,6], models that involve nonlinear diffusion [7], and patch-structured diffusion frameworks [8, 9]. Further related developments can also be found in reaction-diffusion-advection, mobility-related, and steady-state analyses of spatial SIS epidemic models (see [10–14]). Each of these variations captures distinct biological mechanisms and has led to a wide range of dynamical behaviors.

To better reflect the population growth pattern constrained by environmental resources in reality, Li et al. [15] further introduced a logistic population regulation mechanism into the diffusive SIS framework:

$$\begin{cases} S_t = d_S \Delta S + a(x)S - b(x)S^2 - \beta(x)\dfrac{SI}{S+I} + \gamma(x)I, & x \in \Omega,\ t > 0, \\ I_t = d_I \Delta I + \beta(x)\dfrac{SI}{S+I} - \gamma(x)I, & x \in \Omega,\ t > 0, \\ \dfrac{\partial S}{\partial \nu} = \dfrac{\partial I}{\partial \nu} = 0, & x \in \partial\Omega,\ t > 0, \\ S(x,0) = S_0(x), \quad I(x,0) = I_0(x), & x \in \Omega. \end{cases} \tag{1.2}$$

where the growth of the susceptible population is described by the term $a(x)S - b(x)S^2$. This mechanism reflects density-dependent regulation under resource-limited conditions, thereby preventing an unbounded growth of the population size and breaking the structure of total population conservation in the classic SIS model, thus allowing the overall population to evolve over time. Under homogeneous Neumann boundary conditions, the authors proved the global well-posedness of the solution and demonstrated that the basic reproduction number remains the key threshold to determine the extinction and persistence of the disease. Compared with the linear population mechanism, the logistic-type regulation significantly enhances the nonlinear characteristics of the system, alters the spatial structure of the equilibrium state, and increases the sensitivity of the disease spatial spread to the diffusion intensity and environmental parameters, thereby presenting more complex dynamical behaviors. Relevant studies can be found in [16–18] and the references therein.

In real epidemic situations, several additional factors may also affect disease transmission. Examples include reducing effective contact through the isolation of infected individuals [19], blocking transmission chains by contact tracing and selective quarantine [20], lowering infection risk by medical treatment under limited capacity [21], and decreasing the number of infectives through a constant removal rate [22]. Although these strategies arise from different public health considerations, they can all be mathematically interpreted as mechanisms that remove individuals from the disease transmission process within the habitat. This naturally raises the question of how to model boundary outflow in a spatial epidemic system.

In this direction, Hu et al., [23] explored an SIS evolutionary system characterized by Robin boundary settings. This framework incorporates the emigration of both susceptible and infectious individuals via the domain boundary. Their model is given by the following:

$$\begin{cases} S_t = d_S \Delta S + \Lambda(x) - S - \beta(x)\dfrac{SI}{S+I} + \theta\gamma(x)I, & x \in \Omega,\ t > 0, \\ I_t = d_I \Delta I + \beta(x)\dfrac{SI}{S+I} - \gamma(x)I, & x \in \Omega,\ t > 0, \\ \dfrac{\partial S}{\partial n} = -aS, \quad \dfrac{\partial I}{\partial n} = -bI, & x \in \partial\Omega,\ t > 0, \\ S(x,0) = S_0(x) \geq 0, \quad I(x,0) = I_0(x) \geq 0,\ I_0 \not\equiv 0, & x \in \Omega. \end{cases} \tag{1.3}$$

The positive constants a and b quantify the emigration strengths of the susceptible and infected populations at the boundary, respectively. $\theta \in (0,1)$ represents the fraction of recovered infected individuals who return to the susceptible class. Under this mechanism, the boundary outflow has a significant impact on the long-term behavior of disease transmission: When the outflow rate of infected individuals exceeds a critical threshold b^*, the disease dies out, whereas insufficient outflow leads to uniform persistence, with spatial diffusion and environmental heterogeneity further enhancing the transmission potential.

Recent progress expands the analysis of spatial SIS epidemic models with boundary settings or movement-related mechanisms. For example, Wang et al. [24] discussed a spatially heterogeneous reaction-diffusion SIS model that uses general nonlinear incidence functions and Dirichlet boundary conditions, and obtained its threshold dynamics based on the basic reproduction number. Hu et al., [25] investigated another SIS reaction-diffusion model including specific control areas where no new infections appear, and explained how such spatial control areas stop diseases from lasting. Besides, Salako and Wu [26] studied a patch-based epidemic model with mass-action transmission and asymmetric diffusion rules, and found how the movement links among different patches affect disease survival and endemic steady states. All these existing studies point out that boundary effects, spatial control, and patch connections greatly matter in epidemic dynamics.

Based on the above two types of studies, this paper investigates the interaction between the logistic population regulation and the boundary outflow in the SIS infectious disease model under spatial heterogeneity. We consider a class of reaction-diffusion type SIS systems, where susceptible individuals are regulated by the nonlinear logistic term $S(\rho(x)-\mu(x)S)$, and both susceptible and infected individuals can migrate out of the habitat through the Robin boundary under the Robin boundary condition. Compared with the model in [15], the introduction of boundary outflow breaks the total population conservation structure, thus bringing new difficulties in the global dynamical analysis; while compared with the situation in [23] that only contains a linear population mechanism, the logistic nonlinear regulation further changes the equilibrium structure, and imposes higher requirements on the dissipativity, and the solutions to Eq (2.1) remain uniformly bounded over the entire domain. From a mathematical perspective, the main challenge lies in establishing clear threshold criteria in an open system, because at this time, the total population is neither conserved nor controlled by the linear population term, and it is not immediately clear whether the reproductive index derived from the linearized framework retains its threshold role in characterizing the disease's elimination or endemic prevalence. By combining spectral analyses and the monotone dynamical system theory, this paper proves that when both logistic regulation and boundary outflow are simultaneously introduced, the classical threshold principle still holds.

The structure arrangement of this article are summarized as follows. Section 2 constructs the model and proves the global uniqueness, positivity, and uniform boundedness of the solution. Section 3 introduces the basic reproduction number $\mathcal{R}_0$ through the spectral analysis of the linearized system at the disease-free equilibrium point, and shows that it still characterizes the threshold feature of disease transmission. Section 4 explores the global dynamics, thereby demonstrating that the disease-free state retains global asymptotic stability provided that $\mathcal{R}_0 < 1$; in contrast, the condition $\mathcal{R}_0 > 1$ ensures that the disease becomes uniformly permanent, thus leading to the existence of at least one endemic stationary point. Section 5 discusses the impact of boundary population outflow, and the results show that the outflow of susceptible individuals does not change the threshold $\mathcal{R}_0$, but will affect the spatial distribution and scale of the equilibrium state; conversely, the outflow of infected individuals plays a key role in disease control, which can effectively reduce $\mathcal{R}_0$ and expand the parameter range for disease extinction. Finally, Section 6 presents the core findings of the entire paper and provides biological explanations and discussions.

2. The model

2.1. The basic properties

In the following framework, we assume $\Omega \subset \mathbb{R}^N$ ($N \geq 1$) is a bounded habitat with a smooth boundary $\partial\Omega$, where ν represents the outward unit normal. Additionally we also assume that ρ, μ, β, and γ in $C^{\alpha}(\bar{\Omega})$, $\rho(x)$, $\mu(x)$, $\beta(x)$, $\gamma(x) > 0$ for $x \in \bar{\Omega}$, for some $0 < \alpha < 1$. Moreover, $d_S > 0$, $d_I > 0$, $a \geq 0$, $b \geq 0$, and $0 < \theta \leq 1$. The standard incidence term is defined by continuity at the origin, namely $\frac{SI}{S+I} = 0$ when $S = I = 0$.

We consider two population densities, $S(x,t)$ and $I(x,t)$, which represent susceptible and infected individuals, respectively, at spatial location $x \in \Omega$ and time $t > 0$. The movement of both populations is governed by diffusion processes with constant diffusion coefficients d_S and d_I. The disease dynamics are governed by a standard incidence rate $\beta(x)$ alongside a recovery rate $\gamma(x)$, both of which are spatially dependent. The interpretation of the parameter θ and the initial distributions $S_0(x), I_0(x)$ remains consistent with the aforementioned models. Specifically, we examine the following system:

$$\begin{cases} S_t = d_S \Delta S + S(\rho(x) - \mu(x)S) - \beta(x)\dfrac{SI}{S+I} + \theta\gamma(x)I, & x \in \Omega,\ t > 0, \\ I_t = d_I \Delta I + \beta(x)\dfrac{SI}{S+I} - \gamma(x)I, & x \in \Omega,\ t > 0, \\ \dfrac{\partial S}{\partial \nu} + aS = 0, \quad \dfrac{\partial I}{\partial \nu} + bI = 0, & x \in \partial\Omega,\ t > 0, \\ S(x,0) = S_0(x) \geq 0, \quad I(x,0) = I_0(x) \geq 0,\ I_0 \not\equiv 0, & x \in \Omega, \end{cases} \tag{2.1}$$

where $\mu(x)$ represents the strength of the logistic crowding effect (density-dependent regulation) acting on the susceptible population at location $x \in \overline{\Omega}$. Our framework incorporates the assumption that the entire population density is governed by a logistic regulation and there is a population outflow on the boundary. The term $S(\rho(x) - \mu(x)S)$ describes the logistic-type regulation of the total population. When $I \equiv 0$, the susceptible population follows a logistic equation with spatial heterogeneity. The Robin boundary conditions in Eq (2.1) reflect individuals can flow out at the boundaries, with a and b representing the per capita outward flux rates of susceptibles and infecteds, respectively. These two rates are allowed to differ because susceptible individuals may leave the habitat through ordinary migration or commuting, whereas infected individuals may be removed from the local transmission process through quarantine, hospitalization, medical transfer, or other control measures. Accordingly, parameter b is interpreted not only as the natural outward migration rate of infected individuals, but also as the effective boundary-mediated removal rate induced by epidemic containment measures.

In this section, we summarize several fundamental properties of System (2.1). The proofs can be carried out by standard arguments for parabolic systems.

Lemma 1. *Given any initial data* $(S_0, I_0) \in [C(\overline{\Omega})]^2$ *that is non-negative and non-null with* $I_0 \not\equiv 0$*, the reaction-diffusion framework* (2.1) *possesses a unique classical solution defined locally in time satisfying*

$$S, I \in C^{2,1}(\overline{\Omega} \times (0, T_{\max})) \cap C(\overline{\Omega} \times [0, T_{\max})),$$

and

$$S(x,t) > 0, \quad I(x,t) > 0, \quad \forall\, x \in \overline{\Omega},\ t \in (0, T_{\max}).$$

Proof. Since the reaction terms are locally Lipschitz and the boundary conditions are linear of the Robin type, the standard parabolic theory ensures the local existence and uniqueness of a classical solution (see, e.g., [27, Chapter 6]). Starting from nonnegative initial data, the nonnegative cone is invariant by the parabolic comparison principle. Moreover, since $I_0 \not\equiv 0$ and $\theta \in (0,1)$, the strong maximum principle together with the Hopf boundary lemma yields $S(x,t) > 0$ and $I(x,t) > 0$ for all $x \in \overline{\Omega}$ and $t \in (0, T_{\max})$.

Lemma 2. *Under the above assumptions, there exists a constant $C > 0$ only depending on the parameters and the domain, such that any solution (S, I) of Eq (2.1) satisfies the following:*

$$0 \le S(x,t) + I(x,t) \le C, \quad \forall x \in \overline{\Omega},\ t \ge 0.$$

Proof. Let $N(x,t) = S(x,t) + I(x,t)$. Summing the equations in Eq (2.1), we obtain the following:

$$N_t = \Delta(d_S S + d_I I) + S(\rho(x) - \mu(x)S) - (1-\theta)\gamma(x)I. \tag{2.2}$$

Since $0 < \theta < 1$ and $I \ge 0$, we have $-(1-\theta)\gamma(x)I \le 0$. Moreover, the logistic term $f(S) = S(\rho(x) - \mu(x)S)$ is bounded from above by $M = \max_{x\in\overline{\Omega}} \frac{\rho^2(x)}{4\mu(x)}$. Thus, N satisfies the following differential inequality in the sense of distributions:

$$N_t \le \Delta(d_S S + d_I I) + M.$$

Given the Robin boundary conditions $\partial_\nu S + aS = 0$ and $\partial_\nu I + bI = 0$ with $a, b \ge 0$, it follows that $\partial_\nu(d_S S + d_I I) \le 0$. By standard parabolic regularity and L^p estimates for dissipative systems (see, e.g., [27, Theorem 3.1]), the uniform boundedness of $N(x,t)$ is maintained for all $t \in (0, T_{\max})$.

To provide an explicit bound C, we can refine the argument as follows. Since N is bounded, I is also bounded. Then, S satisfies the following:

$$S_t \le d_S \Delta S + S(\rho_{\max} - \mu_{\min} S) + \theta\gamma_{\max}\|I\|_\infty.$$

The quadratic term $-\mu_{\min}S^2$ ensures that S is bounded by some constant C_1. Subsequently, from the I-equation, we have the following:

$$I_t \le d_I \Delta I + \beta_{\max} S - \gamma_{\min} I \le d_I \Delta I + \beta_{\max} C_1 - \gamma_{\min} I. \tag{2.3}$$

Let $z(t)$ be the solution to the ordinary differential equation (ODE):

$$\dot{z} = \beta_{\max} C_1 - \gamma_{\min} z, \quad z(0) = \|I_0\|_{L^\infty}.$$

Then, $z(t) \le \max\left\{\|I_0\|_{L^\infty}, \frac{\beta_{\max} C_1}{\gamma_{\min}}\right\} =: C_2$. By the comparison principle, $I(x,t) \le C_2$.

By combining the bounds for S and I, we obtain $\|S(\cdot,t)\|_{L^\infty} + \|I(\cdot,t)\|_{L^\infty} \le C_1 + C_2 =: C$. Then, the standard continuation argument for parabolic systems implies $T_{\max} = +\infty$, thus completing the proof.

Theorem 1. *Under the assumptions of Lemmas 1 and 2, for any nonnegative initial data $(S_0, I_0) \in [C(\overline{\Omega})]^2$ with $I_0 \not\equiv 0$, System (2.1) admits a unique global classical solution (S, I) such that*

$$S, I \in C^{2,1}(\overline{\Omega} \times (0,\infty)) \cap C(\overline{\Omega} \times [0,\infty)),$$

and

$$S(x,t) > 0,\ I(x,t) > 0 \ \textit{for all } x \in \overline{\Omega} \textit{ and } t > 0.$$

Proof. By Lemma 1, the system admits a unique, strictly positive local classical solution (S, I) on the maximal interval $[0, T_{\max})$. In view of Lemma 2, there exists a uniform bound $M > 0$, independent of $T_{\max}$, such that

$$\|S(\cdot,t)\|_{L^\infty} + \|I(\cdot,t)\|_{L^\infty} \le M, \quad \forall t \in [0, T_{\max}).$$

By the standard continuation principle for reaction-diffusion systems (see, e.g., [27]), the local solution can be extended globally in time, (i.e., $T_{\max} = +\infty$.) The uniqueness and continuous dependence on initial data follow from the standard parabolic theory. Similar arguments for related spatial epidemic models can be found in [1, 28]. The proof is complete.

2.2. *The disease-free equilibrium (DFE)*

Next, We explore the time-independent profiles $(\tilde{S}, \tilde{I})$ of System (2.1), which are obtained by solving the underlying semilinear elliptic system:

$$\begin{cases} d_S \Delta \tilde{S} + \tilde{S}(\rho(x) - \mu(x)\tilde{S}) - \beta(x)\dfrac{\tilde{S}\,\tilde{I}}{\tilde{S}+\tilde{I}} + \theta\gamma(x)\tilde{I} = 0, & x \in \Omega, \\ d_I \Delta \tilde{I} + \beta(x)\dfrac{\tilde{S}\,\tilde{I}}{\tilde{S}+\tilde{I}} - \gamma(x)\tilde{I} = 0, & x \in \Omega, \\ \dfrac{\partial \tilde{S}}{\partial \nu} + a\tilde{S} = 0, \quad \dfrac{\partial \tilde{I}}{\partial \nu} + b\tilde{I} = 0, & x \in \partial\Omega. \end{cases} \tag{2.4}$$

Throughout this section, we only consider nonnegative equilibria. First, We consider the semi-trivial state of the system. By setting the infection density to zero (i.e., $\tilde{I} \equiv 0$), the first equation in System (2.4) reduces into a single elliptic equation of the logistic variety as follows:

$$\begin{cases} d_S \Delta S + S(\rho(x) - \mu(x)S) = 0, & x \in \Omega, \\ \dfrac{\partial S}{\partial \nu} + aS = 0, & x \in \partial\Omega. \end{cases} \tag{2.5}$$

Before studying the disease-free equilibrium, we first introduce the principal eigenvalue associated with the linearization of the susceptible logistic equation at the trivial steady state. For each $a \ge 0$, let $\lambda_S(a)$ be the principal eigenvalue of

$$\begin{cases} d_S \Delta \phi + \rho(x)\phi = \lambda\phi, & x \in \Omega, \\ \dfrac{\partial \phi}{\partial \nu} + a\phi = 0, & x \in \partial\Omega. \end{cases} \tag{2.6}$$

Equivalently,

$$\lambda_S(a) = \sup_{0 \ne \phi \in H^1(\Omega)} \frac{-d_S \displaystyle\int_\Omega |\nabla\phi|^2\,dx - a d_S \int_{\partial\Omega} \phi^2\,ds + \int_\Omega \rho(x)\phi^2\,dx}{\displaystyle\int_\Omega \phi^2\,dx}.$$

In what follows, we assume that

$$\lambda_S(a) > 0. \tag{2.7}$$

This condition means that the susceptible population can persist in the habitat in the absence of infection.

proposition 1. *Assume that $\rho, \mu \in C(\bar{\Omega})$ and that Eq* (2.7) *holds. Then, the logistic elliptic problem*

$$\begin{cases} d_S \Delta S + S(\rho(x) - \mu(x)S) = 0, & x \in \Omega, \\ \dfrac{\partial S}{\partial \nu} + aS = 0, & x \in \partial\Omega \end{cases} \tag{2.8}$$

admits a unique positive solution $\hat{S}_a \in C^2(\bar{\Omega})$. Consequently, System (2.1) *admits the disease-free equilibrium $(\hat{S}_a, 0)$. Moreover, if $\lambda_S(a) \leq 0$, then Eq* (2.8) *has no positive solution; in this case, its only nonnegative solution is $S \equiv 0$.*

Proof. First, we assume that $\lambda_S(a) > 0$. Let $\phi_S > 0$ be the positive eigenfunction associated with $\lambda_S(a)$. Then, for sufficiently small $\varepsilon > 0$, the function

$$\underline{S} = \varepsilon\phi_S$$

is a positive sub-solution of Eq (2.8). Indeed, using Eq (2.6), we have

$$d_S \Delta \underline{S} + \underline{S}(\rho(x) - \mu(x)\underline{S}) = \varepsilon\lambda_S(a)\phi_S - \mu(x)\varepsilon^2\phi_S^2 > 0,$$

provided that $\varepsilon > 0$ is sufficiently small. Moreover, $\underline{S}$ satisfies the Robin boundary condition.

On the other hand, let

$$K = \frac{\rho_{\max}}{\mu_{\min}}.$$

Then, the constant function $\overline{S} = K$ is a super-solution. In fact,

$$d_S \Delta \overline{S} + \overline{S}(\rho(x) - \mu(x)\overline{S}) = K(\rho(x) - \mu(x)K) \leq 0 \quad \text{in } \Omega,$$

and

$$\frac{\partial \overline{S}}{\partial \nu} + a\overline{S} = aK \geq 0 \quad \text{on } \partial\Omega.$$

Choosing ε smaller if necessary, we may assume $\underline{S} \leq \overline{S}$ in $\bar{\Omega}$. Then the standard method of upper and lower solutions for semilinear elliptic equations with Robin boundary conditions yields a positive solution $\hat{S}_a$ of Eq (2.8) that satisfies the following:

$$0 < \underline{S} \leq \hat{S}_a \leq \overline{S}.$$

Next, we prove uniqueness. Suppose that S_1 and S_2 are two positive solutions of Eq (2.8). Since the nonlinear term

$$f(x, S) = S(\rho(x) - \mu(x)S)$$

is strictly subhomogeneous with respect to $S > 0$, the standard comparison argument for logistic elliptic equations implies $S_1 \equiv S_2$. Therefore, the positive solution is unique.

It remains to show that no positive solution exists when $\lambda_S(a) \leq 0$. By contradiction, assume that $S > 0$ solves Eq (2.8). Let $\phi_S > 0$ be the positive eigenfunction corresponding to $\lambda_S(a)$. Multiplying Eq (2.8) by ϕ_S, multiplying Eq (2.6) by S, integrating over Ω, and subtracting the two identities, using the same Robin boundary condition for S and ϕ_S, we obtain the following:

$$\lambda_S(a) \int_\Omega S\phi_S \, dx = \int_\Omega \mu(x) S^2 \phi_S \, dx.$$

The right-hand side is strictly positive. Hence, $\lambda_S(a) > 0$, which contradicts $\lambda_S(a) \le 0$. Thus, no positive solution exists when $\lambda_S(a) \le 0$.

Finally, if $S \ge 0$ is a nonnegative solution and $S \not\equiv 0$, then the strong maximum principle and the Hopf boundary lemma imply $S > 0$ in $\bar{\Omega}$, which is impossible when $\lambda_S(a) \le 0$. Hence, the only nonnegative solution in this case is $S \equiv 0$. The proof is complete.

remark 1. *The condition $\lambda_S(a) > 0$ is not automatic when the susceptible boundary outflow rate a is large. As a increases, the Robin boundary condition approaches the Dirichlet limiting case, and the principal eigenvalue $\lambda_S(a)$ may become nonpositive. Biologically, the case $\lambda_S(a) \le 0$ corresponds to a strong-outflow regime in which the susceptible population cannot maintain itself in the habitat, even in the absence of infection. Since the main purpose of this paper is to study the epidemic threshold around a nontrivial disease-free equilibrium, we impose $\lambda_S(a) > 0$ throughout the subsequent analysis.*

proposition 2. *Let $\hat{S}(\cdot, a)$ be the unique positive solution of the elliptic problem* (2.5) *corresponding to the boundary outflow rate $a > 0$. If $0 < a_1 < a_2$, then $\hat{S}(\cdot, a_2) < \hat{S}(\cdot, a_1)$ in $\overline{\Omega}$, that the disease-free susceptible steady state is strictly decreasing with respect to the susceptible boundary outflow rate a.*

Proof. Fix $0 < a_1 < a_2$. By definition, $\hat{S}(\cdot, a_i)$ satisfies

$$\begin{cases} d_S \Delta \hat{S}(\cdot, a_i) + \widehat{S}(\cdot, a_i)(\rho(\cdot) - \mu(\cdot)\hat{S}(\cdot, a_i)) = 0, & x \in \Omega, \\ \dfrac{\partial \hat{S}}{\partial \nu}(\cdot, a_i) + a_i \hat{S}(\cdot, a_i) = 0, & x \in \partial\Omega, \end{cases}$$

for $i = 1, 2$.

First we show that $\hat{S}(\cdot, a_2) \le \hat{S}(\cdot, a_1)$. Observe that $\hat{S}(\cdot, a_1)$ satisfies the same elliptic equation in Ω as $\hat{S}(\cdot, a_2)$. To compare them, we consider the boundary operator $\mathcal{B}_a := \frac{\partial}{\partial \nu} + aI$ acting on the boundary $\partial\Omega$. Specifically, for the parameter a_2, a direct evaluation yields

$$B_{a_2}\hat{S}(\cdot, a_1) = (a_2 - a_1)\hat{S}(\cdot, a_1) \ge 0 \quad \text{on } \partial\Omega,$$

which shows that $\hat{S}(\cdot, a_1)$ satisfies the boundary inequality that corresponds to Problem (2.5) with parameter $a = a_2$. Consequently, $\hat{S}(\cdot, a_1)$ serves as a positive super-solution, while the trivial function $S \equiv 0$ is a sub-solution.

By virtue of the sub- and super-solution principle and the uniqueness of the positive solution for any given $a > 0$, it follows that

$$0 < \hat{S}(\cdot, a_2) \le \hat{S}(\cdot, a_1) \quad \text{in } \overline{\Omega}.$$

To verify the strict inequality, suppose on the contrary that $\hat{S}(\cdot, a_2)$ coincides with $\hat{S}(\cdot, a_1)$ at some point $x_0 \in \overline{\Omega}$. Since both functions solve the same elliptic equation in Ω and satisfy $\hat{S}(\cdot, a_2) \le \hat{S}(\cdot, a_1)$ throughout $\overline{\Omega}$, the strong maximum principle combined with Hopf's lemma (see, e.g., [29, 30]) forces

$$\hat{S}(\cdot, a_2) \equiv \hat{S}(\cdot, a_1) \quad \text{in } \overline{\Omega},$$

which contradicts the uniqueness of the solution corresponding to different parameter values. Hence, the inequality must be strict.

However, for $i = 1, 2$, $\hat{S}(\cdot, a_i)$ satisfies the Robin boundary condition

$$\frac{\partial \hat{S}}{\partial \nu}(\cdot, a_i) + a_i \hat{S}(\cdot, a_i) = 0 \quad \text{on } \partial\Omega.$$

If $\hat{S}(\cdot, a_2) \equiv \hat{S}(\cdot, a_1)$, then

$$(a_2 - a_1)\hat{S}(\cdot, a_1) = 0 \quad \text{for all } x \in \partial\Omega,$$

which contradicts $a_2 > a_1$ and $\hat{S}(\cdot, a_1) > 0$ on $\overline{\Omega}$. Therefore, $\hat{S}(\cdot, a_2) < \hat{S}(\cdot, a_1)$, for all $x \in \overline{\Omega}$.

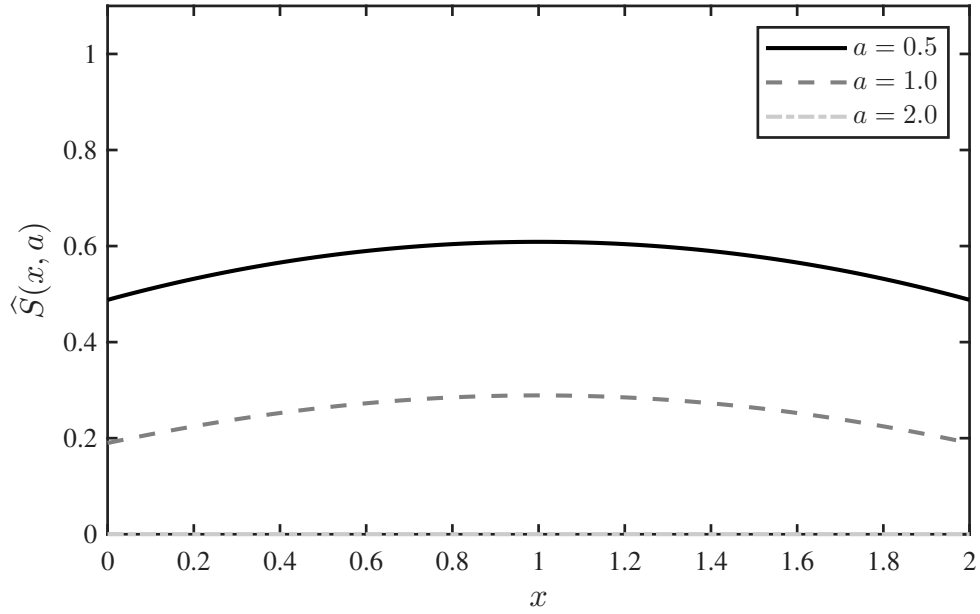

Figure 1. Numerical steady states $\hat{S}(\cdot, a)$ of the one-dimensional logistic model with $d_S = 1$, $\rho = 1$, $\mu = 1$, and $L = 2$.

Although an explicit expression of the positive equilibrium $\hat{S}(\cdot, a)$ is generally unavailable for the nonlinear logistic model, this monotonicity can also be clearly observed from numerical plots of $\hat{S}(\cdot, a)$ for different values of a. To visualize this monotonicity, we consider the one-dimensional domain $(0, L)$ with constant coefficients and numerically solve the boundary formulation of the problem

$$d_S S''(x) + S(\rho - \mu S) = 0, \quad x \in (0, L),$$

with Robin boundary constraints $S'(0) = aS(0)$ and $S'(L) = -aS(L)$.

For the typical choice $d_S = 1$, $\rho = 1$, $\mu = 1$, and $L = 2$, Figure 1 shows the profiles of $\hat{S}(\cdot, a)$ for $a = 0.5, 1.0, 2.0$. As a increases, the entire profile of $\hat{S}(\cdot, a)$ shifts downward, thus confirming the theoretical prediction that $\widehat{S}(\cdot, a)$ strictly decreases as a increases.

3. Spectral analysis and the threshold parameter $\mathcal{R}_0$

3.1. The linearized operator and its eigenvalues

To derive the threshold Parameter $\mathcal{R}_0$, we perform a linearization of the infectious component in System (2.1) around the disease-free state. Under the assumption of a small infectious population I and noting $\hat{S}(x) > 0$, the incidence term is approximated by the following:

$$\beta(x)\frac{\hat{S}I}{\hat{S} + I} \approx \beta(x)I.$$

Consequently, the linearized evolution of I is governed by the following:

$$I_t = d_I \Delta I + (\beta(x) - \gamma(x))I \quad \text{in } \Omega, \qquad \frac{\partial I}{\partial \nu} + bI = 0 \quad \text{on } \partial\Omega. \tag{3.1}$$

The corresponding eigenvalue problem is given by the following:

$$\begin{cases} d_I \Delta \phi + (\beta(x) - \gamma(x))\phi = \lambda \phi, & x \in \Omega, \\ \dfrac{\partial \phi}{\partial \nu} + b\phi = 0, & x \in \partial\Omega. \end{cases} \tag{3.2}$$

By virtue of the Krein-Rutman theory (see, e.g., [31]), the operator in Eq (3.2) possesses a principal eigenvalue λ_1. This eigenvalue is characterized by its reality, algebraic simplicity, and the existence of a corresponding strictly positive eigenfunction $\phi_1 \in C^2(\overline{\Omega})$. The variational representation of λ_1 is given by the following quotient:

$$\lambda_1 = \sup_{0 \neq \phi \in H^1(\Omega)} \left\{ \frac{-d_I \int_\Omega |\nabla \phi|^2 \, dx - b d_I \int_{\partial\Omega} \phi^2 \, ds + \int_\Omega (\beta(x) - \gamma(x)) \, \phi^2 \, dx}{\int_\Omega \phi^2 \, dx} \right\} \tag{3.3}$$

Clearly, the pair (λ_1, ϕ_1) satisfies the boundary value problem (3.2). For the boundary emigration (i.e., $b = 0$), the model simplifies to a standard Neumann-type framework. Let $\widehat{\lambda}$ represent the principal eigenvalue in this simplified scenario, which can be characterized as follows:

$$\widehat{\lambda} := \sup_{0 \neq \phi \in H^1(\Omega)} \left\{ \frac{-d_I \int_\Omega |\nabla \phi|^2 \, dx + \int_\Omega (\beta(x) - \gamma(x)) \phi^2 \, dx}{\int_\Omega \phi^2 \, dx} \right\}. \tag{3.4}$$

From a spectral perspective, if the net growth rate $\beta(x) - \gamma(x)$ is non-positive throughout $\overline{\Omega}$, then $\widehat{\lambda} < 0$ for all $d_I > 0$. However, if $\beta(x) - \gamma(x)$ changes sign and its average value $\int_\Omega (\beta(x) - \gamma(x)) dx$ is positive, then we can define a critical dispersal rate $\widehat{d_I}$ as follows:

$$\widehat{d_I} := \sup_{\phi \in H^1(\Omega), \int_\Omega (\beta - \gamma)\phi^2 > 0} \left\{ \frac{\int_\Omega (\beta(x) - \gamma(x)) \phi^2 \, dx}{\int_\Omega |\nabla \phi|^2 dx} \right\}. \tag{3.5}$$

In this context, the magnitude of d_I relative to $\widehat{d_I}$ dictates the sign of $\widehat{\lambda}$: specifically, $\widehat{\lambda} > 0$ when diffusion is restricted ($d_I < \widehat{d_I}$), while $\widehat{\lambda} < 0$ for high dispersal rates ($d_I > \widehat{d_I}$). These properties arise from the classical theory of self-adjoint elliptic operators.

proposition 3. *Let $b > 0$ be fixed. For an $d_I > 0$, let $\lambda_1(d_I, b)$ be the dominant eigenvalue associated with Eq* (3.3)*, and denote the corresponding strictly positive eigenfunction by $\phi_1(d_I, b)$. Then:*

(1) *$\lambda_1(d_I, b)$ strictly decreases as the diffusion rate d_I increases, and*

$$\frac{\partial \lambda_1}{\partial d_I} = -\frac{\displaystyle\int_\Omega |\nabla \phi_1|^2 \, dx + \int_{\partial\Omega} b(\phi_1)^2 \, ds}{\displaystyle\int_\Omega (\phi_1)^2 \, dx} < 0.$$

(2) *We have*

$$\lim_{d_I\to 0^+}\lambda_1(d_I,b)=\sup_{x\in\Omega}(\beta(x)-\gamma(x)),\ \lim_{d_I\to+\infty}\lambda_1(d_I,b)=-\infty.$$

(3) *Assume $\beta(x)-\gamma(x)$ changes sign in Ω and satisfies $\int_\Omega(\beta-\gamma)\,dx>0$. Then, there exists a unique critical value $d_I^1>0$ such that $\lambda_1(d_I^1,b)=0$. Specifically, the spectral sign is determined as:*

$$\lambda_1(d_I,b)>0 \text{ for } 0<d_I<d_I^1,\quad \lambda_1(d_I,b)<0 \text{ for } d_I>d_I^1,$$

and d_I^1 is given by

$$d_I^1:=\sup_{\substack{\phi\in H^1(\Omega),\,\phi\not\equiv 0\\ \int_\Omega(\beta-\gamma)\phi^2\,dx>0}}\left\{\frac{\displaystyle\int_\Omega(\beta(x)-\gamma(x))\phi^2\,dx}{\displaystyle\int_\Omega|\nabla\phi|^2\,dx+b\int_{\partial\Omega}\phi^2\,ds}\right\}. \tag{3.6}$$

Proof. We only prove Assertion (1). For brevity, we write $\lambda_1(d_I,b)=:\lambda_1,\phi_1(d_I,b)=:\phi_1$. Differentiate Eq (3.3) with respect to d_I. By writing $\psi:=\partial_{d_I}\phi_1$, we obtain the following:

$$\begin{cases}\Delta\phi_1+d_I\Delta\psi+(\beta(x)-\gamma(x))\psi=\partial_{d_I}\lambda_1\phi_1+\lambda_1\psi, & x\in\Omega,\\ \dfrac{\partial\psi}{\partial\nu}+b\psi=0, & x\in\partial\Omega.\end{cases} \tag{3.7}$$

Multiply Eq (3.7) by ϕ_1, multiply Eq (3.2) by ψ, integrate over Ω, and subtract the two identities. After an integration by parts, the terms that involve ψ cancel thanks to the same Robin boundary condition for ϕ_1 and ψ. This yields

$$\frac{\partial\lambda_1}{\partial d_I}=-\frac{\displaystyle\int_\Omega|\nabla\phi_1|^2\,dx+\int_{\partial\Omega}b\phi_1^2\,ds}{\displaystyle\int_\Omega\phi_1^2\,dx}<0,$$

because $\phi_1>0$ in Ω, $b>0$. Hence, $\lambda_1(d_I,b)$ is strictly decreasing in d_I. (2) and (3) can be obtained from the variational arguments; for brevity, we forgo the exhaustive details and cite [23, 32] for analogous proofs.

proposition 4. *Let d_I be fixed. For any $b>0$, denote the principal eigenvalue of problem* (3.3) *by $\lambda_1(d_I,b)$, with the associated eigenfunction ϕ_1. Then:*

(1) *$\lambda_1(d_I,b)$ strictly decreases as the boundary outflow rate b increases, and*

$$\frac{\partial\lambda_1}{\partial b}=-\frac{\displaystyle\int_{\partial\Omega}d_I(\phi_1)^2\,ds}{\displaystyle\int_\Omega(\phi_1)^2\,dx}<0.$$

(2) *Let $\widehat{\lambda}(d_I)$ and $\lambda^D(d_I)$ be the principal eigenvalues of the Neumann and Dirichlet problems associated with Eq* (3.3)*, respectively. Then,*

$$\lim_{b\to 0^+}\lambda_1(d_I,b)=\widehat{\lambda}(d_I),\quad \lim_{b\to+\infty}\lambda_1(d_I,b)=\lambda^D(d_I).$$

In particular, the map $b \mapsto \lambda_1(d_I, b)$ is continuous on $[0, +\infty)$ and

$$\lambda^D(d_I) \le \lambda_1(d_I, b) \le \widehat{\lambda}(d_I) \quad \text{for all } b > 0.$$

Moreover, if $\lambda^D(d_I) > 0$, then $\lambda_1(d_I, b) > 0$ for all $b > 0$.

(3) *Moreover, assume that $\widehat{\lambda}(d_I) > 0 > \lambda^D(d_I)$. Consequently, the eigenvalue $\lambda_1(d_I, b)$ possesses a unique positive zero b_1. Furthermore, its sign is strictly determined by the magnitude of b relative to this critical threshold b_1:*

$$\lambda_1(d_I, b) < 0 \quad \text{for } b > b_1, \quad \lambda_1(d_I, b) > 0 \quad \text{for } 0 < b < b_1.$$

Furthermore, b_1 admits the variational representation

$$b_1 := \sup_{\substack{\phi \in H^1(\Omega),\, \phi \not\equiv 0 \\ \int_\Omega [(\beta-\gamma)\phi^2 - d_I|\nabla\phi|^2]\,dx > 0}} \left\{ \frac{\displaystyle\int_\Omega (\beta(x) - \gamma(x))\phi^2\,dx - d_I \int_\Omega |\nabla\phi|^2\,dx}{\displaystyle d_I \int_{\partial\Omega} \phi^2\,ds} \right\} \tag{3.8}$$

and b_1 decreases strictly as d_I increases.

(4) Assume that the net growth rate $\beta(x) - \gamma(x)$ exhibits sign-changing behavior within Ω and satisfies the integral condition $\int_\Omega (\beta(x) - \gamma(x))\,dx > 0$. Let $\widehat{d_I}$ be the diffusion threshold defined in Eq (3.5). Then:

(a) When $d_I > \widehat{d_I}$, we have

$$\lambda_1(d_I, b) < 0 \quad \text{for all } b > 0.$$

(b) When $d_I < \widehat{d_I}$ and $\lambda^D(d_I) < 0$, then

$$\lambda_1(d_I, b) < 0 \text{ for } b > b_1(d_I), \quad \lambda_1(d_I, b) > 0 \text{ for } 0 < b < b_1(d_I).$$

Proof. (1). For brevity, we write $\lambda_1 = \lambda_1(d_I, b)$ and $\phi_1 = \phi_1(d_I, b)$. Differentiate Eq (3.3) with respect to b. By writing $\tilde{\psi} := \partial_b \phi_1$, we obtain the following:

$$\begin{cases} d_I \Delta\tilde{\psi} + (\beta(x) - \gamma(x))\tilde{\psi} = \partial_b\lambda_1\phi_1 + \lambda_1\tilde{\psi}, & x \in \Omega, \\ \dfrac{\partial\tilde{\psi}}{\partial\nu} + \phi_1 + b\tilde{\psi} = 0, & x \in \partial\Omega. \end{cases} \tag{3.9}$$

Multiply Eq (3.9) by ϕ_1, multiply Eq (3.2) by $\tilde{\psi}$, integrate over Ω, and subtract the two identities; By applying the same methodology employed in Proposition 3.1 (1), one obtains

$$\frac{\partial\lambda_1}{\partial b} = -\frac{\int_{\partial\Omega} d_I(\phi_1)^2\,ds}{\displaystyle\int_\Omega (\phi_1)^2\,dx} < 0,$$

because $\phi_1 > 0$ in Ω, $d_I > 0$. Hence, $\lambda_1(d_I, b)$ is strictly decreasing in b. This proves (1).

(2). Recall the variational characterization of $\lambda_1(d_I, b)$ given in Eq (3.3). Letting $b \to 0^+$, the boundary term vanishes and the above quotient reduces to that corresponding to the Neumann problem. Hence, $\lambda_1(d_I, b) \to \widehat{\lambda}(d_I)$ as $b \to 0^+$. Since $H_0^1(\Omega) \subset H^1(\Omega)$, it follows that

$$\lambda_1(d_I, b) \geq \sup_{0 \neq \phi \in H_0^1(\Omega)} \frac{-d_I \int_\Omega |\nabla \phi|^2 \, dx + \int_\Omega (\beta(x) - \gamma(x)) \phi^2 \, dx}{\int_\Omega \phi^2 \, dx} = \lambda^D(d_I).$$

Moreover, the limiting behavior of the Robin eigenvalue as $b \to +\infty$ is consistent with the Dirichlet case, a result formally documented in [31]. Therefore, $\lambda_1(d_I, b) \to \lambda^D(d_I)$ as $b \to +\infty$. The two-sided estimate and the continuity immediately follow.

(3). Under the assumption $\widehat{\lambda}(d_I) > 0 > \lambda^D(d_I)$ and by (2), we have the following:

$$\lambda_1(d_I, 0) = \widehat{\lambda}(d_I) > 0, \quad \lambda_1(d_I, b) \to \lambda^D(d_I) < 0 \quad \text{as } b \to +\infty.$$

Due to the continuous and strictly decreasing dependence of the principal eigenvalue on b, as shown in (1), the existence of a unique positive root b_1 is a direct consequence of the intermediate value theorem. From this, the sign characterization of $\lambda_1(d_I, b)$ for $b \neq b_1$ is established at once.

Finally, setting $\lambda_1(d_I, b_1) = 0$ in the quotient for $\lambda_1(d_I, b)$ and rearranging the terms yields the representation Eq (3.8) for b_1. Differentiating $\lambda_1(d_I, b_1) = 0$ with respect to d_I and using Proposition 3 shows that $\partial b_1 / \partial d_I < 0$, (i.e., b_1 is strictly decreasing with respect to d_I). We omit the routine details.

(4). Under the assumption that $\beta(x) - \gamma(x)$ changes sign on Ω and $\int_\Omega (\beta - \gamma) \, dx > 0$, Proposition 3 ensures the occurrence of a critical diffusion threshold $\widehat{d_I} > 0$. This threshold dictates the spectral sign of $\widehat{\lambda}(d_I)$—the principal eigenvalue of Eq (3.3)—such that $\widehat{\lambda}(d_I) > 0$ when $d_I < \widehat{d_I}$ and $\widehat{\lambda}(d_I) < 0$ for $d_I > \widehat{d_I}$. Recall from Proposition 3 that, for each fixed $d_I > 0$, the principal eigenvalue $\lambda_1(d_I, b)$ of the Robin problem satisfies

$$\lambda_1(d_I, 0) = \widehat{\lambda}(d_I), \quad \lambda_1(d_I, b) \to \lambda^D(d_I) \quad \text{as } b \to +\infty,$$

continuously varies, and shows strict monotonicity relative to the parameter $b > 0$.

(a) If $d_I > \widehat{d_I}$, then $\widehat{\lambda}(d_I) < 0$. From part (2), we know that $\lambda_1(d_I, b) \leq \widehat{\lambda}(d_I)$ for all $b > 0$. Hence, $\lambda_1(d_I, b) < 0$ for all $b > 0$.

(b) If $d_I < \widehat{d_I}$ and $\lambda^D(d_I) < 0$, then $\lambda^D(d_I) < 0 < \widehat{\lambda}(d_I)$. Owing to the continuity and strict monotonicity of $\lambda_1(d_I, \cdot)$ with respect to b, the existence of a unique positive zero $b_1(d_I)$ is guaranteed by the identity $\lambda_1(d_I, b_1) = 0$. Consequently, the sign behavior of $\lambda_1(d_I, b)$ for $b \neq b_1(d_I)$ follows the characterization given in (b), the variational characterization Eq (3.8) for $b_1(d_I)$ from Proposition 4, the proof of (4) is finalized.

3.2. The basic reproduction number $\mathcal{R}_0$

definition 1. *Following the next-generation operator framework developed for diffusive epidemic models (see, e.g., [33]), we formulate the basic reproduction number $\mathcal{R}_0$ of System* (2.1) *as the spectral radius of the linearized operator associated with the infection component in Eq* (2.1)*. In the present Robin boundary setting, the following variational characterization is obtained from the corresponding Robin eigenvalue problem:*

$$\mathcal{R}_0 := \sup_{\phi \in H^1(\Omega),\, \phi \neq 0} \frac{\displaystyle\int_\Omega \beta(x) \phi^2 \, dx}{\displaystyle d_I \int_\Omega |\nabla \phi|^2 \, dx + b d_I \int_{\partial\Omega} \phi^2 \, ds + \int_\Omega \gamma(x) \phi^2 \, dx}. \tag{3.10}$$

According to the general spectral theory (see, e.g., [33]), the threshold indicator $\mathcal{R}_0 - 1$is sign-equivalent to the leading eigenvalue λ_1 corresponding to the linearized operator Eq (3.2), that is,

$$sign(\mathcal{R}_0 - 1) = sign(\lambda_1).$$

For later use, we introduce the basic reproduction numbers which correspond to different boundary conditions. When the boundary outflow is absent ($b = 0$), the system obeys the homogeneous Neumann boundary condition. Let $\widehat{\lambda}(d_I)$ be the principal eigenvalue defined in Eq (3.4). We define the corresponding basic reproduction number $\widehat{\mathcal{R}_0}$ such that

$$sign(\widehat{\mathcal{R}_0} - 1) = sign(\widehat{\lambda}).$$

Similarly, let λ^D be the principal eigenvalue of the Dirichlet realization of Eq (2.1),

We denote the corresponding basic reproduction number by $\widehat{\mathcal{R}_0^D}$.

proposition 5. *In view of the R_0 formulation in Definition 1, the following ensuing properties are satisfied:*

(1) $\lambda_1 > 0$ *corresponds to* $\mathcal{R}_0 > 1$, *while* $\lambda_1 < 0$ *corresponds to* $\mathcal{R}_0 < 1$. *Consequently, the infection-free steady state* $(\widehat{S}, 0)$ *undergoes a loss of linear stability when* $\mathcal{R}_0 > 1$.

(2) *For each fixed* $b \geq 0$, $\mathcal{R}_0(d_I, b)$ *decreases as* d_I *increases. Moreover, if* $d_I^1 > 0$ *denotes the unique diffusion threshold given by Proposition 3, then*

$$\mathcal{R}_0(d_I, b) > 1 \quad for\ 0 < d_I < d_I^1, \quad \mathcal{R}_0(d_I, b) < 1 \quad for\ d_I > d_I^1,$$

and

$$\lim_{d_I \to 0^+} \mathcal{R}_0(d_I, b) = \max_{x \in \overline{\Omega}} (\beta(x)/\gamma(x)), \quad \lim_{d_I \to +\infty} \mathcal{R}_0(d_I, b) = 0.$$

(3) *For each fixed* $d_I > 0$, $R_0(d_I, b)$ *decreases as b increases. If* $b_1 > 0$ *is the unique boundary-outflow threshold given by Proposition 4, then*

$$\mathcal{R}_0(d_I, b) > 1 \quad for\ 0 < b < b_1, \quad \mathcal{R}_0(d_I, b) < 1 \quad for\ b > b_1.$$

and

$$\lim_{b \to 0^+} \mathcal{R}_0(d_I, b) = \hat{R}_0, \quad \lim_{b \to +\infty} \mathcal{R}_0(d_I, b) = \mathcal{R}_0^D.$$

(4) The sign of the Dirichlet eigenvalue λ^D provides further information on $\mathcal{R}_0$.

(a) If $\lambda^D > 0$, then $\mathcal{R}_0 > 1$ for all $b > 0$.

(b) If $\lambda^D < 0$ and $\displaystyle\int_\Omega \beta(x)\,dx \leq \int_\Omega \gamma(x)\,dx$, then $\mathcal{R}_0 > 1$ for $0 < b < b_1(d_I)$ and $\mathcal{R}_0 < 1$ for $b > b_1(d_I)$.

(5) Assume that $\beta(x) - \gamma(x)$ changes sign on Ω and $\displaystyle\int_\Omega \beta(x)\,dx > \int_\Omega \gamma(x)\,dx$. The diffusion threshold $\widehat{d_I}$ yields the following classification:

(a) If $d_I > \widehat{d_I}$, then $\mathcal{R}_0 < 1$ for all $b > 0$.

(b) If $d_I < \widehat{d_I}$ and $\lambda^D < 0$, then $\mathcal{R}_0 < 1$ for $b > b_1(d_I)$ and $\mathcal{R}_0 > 1$ for $0 < b < b_1(d_I)$.

These statements are immediate consequences of Propositions 3.1 and 3.2, combined with standard arguments used in [1]. Therefore we omit the details.

4. Global dynamics and the threshold parameter

4.1. Stability analysis of the DFE

Now, we explore the limiting dynamics dictated by the threshold parameter $\mathcal{R}_0$.

Theorem 2. *Provided that $\mathcal{R}_0 < 1$, any solution $(S, I) \in [C(\overline{\Omega})]^2$ to Eq (2.1) with initial data that is non-negative and not identically zero converges to the infection-free steady state $(\hat{S}, 0)$ as $t \to \infty$, that is,*

$$(S(\cdot, t), I(\cdot, t)) \xrightarrow{t\to\infty} (\hat{S}, 0).$$

Proof. In view of Proposition 5, $\lambda_1 < 0$ provided that $\mathcal{R}_0 < 1$. Let $\phi_1 > 0$ be its associated principal eigenfunction. If we weigh the I-equation in Eq (2.1) by ϕ_1 and integrate the result over the spatial domain Ω, we find that

$$\begin{aligned}\frac{d}{dt}\int_\Omega I\phi_1\,dx &= d_I\int_\Omega \Delta I\phi_1\,dx + \int_\Omega\Big(\beta(x)\frac{S}{S+I} - \gamma(x)\Big)I\phi_1\,dx\\ &\le d_I\int_\Omega \Delta I\phi_1\,dx + \int_\Omega(\beta(x)-\gamma(x))I\phi_1\,dx.\end{aligned}$$

Using Robin boundary constrains, we can obtain the following:

$$\frac{\partial I}{\partial \nu} = -bI, \quad \frac{\partial \phi_1}{\partial \nu} = -b\phi_1.$$

Substituting these relations into the boundary term in Green's identity, we obtain the following:

$$I\,\frac{\partial \phi_1}{\partial \nu} - \phi_1\,\frac{\partial I}{\partial \nu} = I(-b\phi_1) - \phi_1(-bI) = -bI\phi_1 + bI\phi_1 = 0.$$

Therefore,

$$\int_\Omega I\,\Delta\phi_1\,dx = \int_\Omega \phi_1\,\Delta I\,dx.$$

Using the eigenvalue identity

$$d_I\Delta\phi_1 + (\beta(x)-\gamma(x))\phi_1 = \lambda_1\phi_1, \quad \frac{\partial\phi_1}{\partial\nu} = -b\phi_1 \quad \text{on } \partial\Omega,$$

and employing integration by parts, we deduce that

$$\frac{d}{dt}\int_\Omega I\phi_1\,dx \le \lambda_1\int_\Omega I\phi_1\,dx. \tag{4.1}$$

Due to $\lambda_1 < 0$, Gronwall's inequality yields the following:

$$\int_\Omega I(\cdot,t)\phi_1(x)\,dx \le Ce^{\lambda_1 t} \to 0 \quad \text{as } t\to\infty.$$

Using $\phi_1 > 0$ on $\overline{\Omega}$ and a standard parabolic regularity, the L^1 convergence implies the following uniform convergence:

$$\|I(\cdot,t)\|_{C(\overline{\Omega})} \to 0 \quad \text{as } t\to\infty.$$

We subsequently establish the limiting behavior of $S(\cdot,t)$. Since $I(\cdot,t) \to 0$ uniformly and the infection component remains bounded, the S-subsystem in Eq (2.1) satisfies the following:

$$S_t = d_S \Delta S + S(\rho(x) - \mu(x)S) + o(1), \tag{4.2}$$

where $o(1)$ represents the term $-\beta\frac{SI}{S+I} + \theta\gamma I$, which vanishes as $t \to \infty$. By invoking the comparison theorem for parabolic operators, one obtains that given each $\varepsilon > 0$, there is a corresponding moment $T(\varepsilon)$ beyond which every solution satisfies the following:

$$\underline{S}_\varepsilon(\cdot) \le S(\cdot,t) \le \overline{S}_\varepsilon(\cdot), \tag{4.3}$$

where $\underline{S}_\varepsilon$ and $\overline{S}_\varepsilon$ are the sole positive solutions of :

$$d_S \Delta S + S(\rho(x) - \mu(x)S) = \pm\varepsilon, \quad \mathcal{B}S = 0. \tag{4.4}$$

and satisfy

$$\|\overline{S}_\varepsilon - \hat{S}\|_{C(\overline{\Omega})} \to 0, \quad \|\underline{S}_\varepsilon - \hat{S}\|_{C(\overline{\Omega})} \to 0 \quad \text{as } \varepsilon \to 0.$$

Letting $\varepsilon \to 0$ gives the following:

$$\lim_{t\to\infty} \|S(\cdot,t) - \hat{S}\|_{C(\overline{\Omega})} = 0.$$

4.2. Uniform persistence and endemic states

The following analysis is devoted to the dynamical behavior when $\mathcal{R}_0 > 1$. Our objective is to demonstrate that the infection will not vanish and to confirm the emergence of at least one steady-state endemic solution.

definition 2. *The epidemic is said to exhibit uniform persistence if one can find a positive threshold $\eta > 0$, such that for every initial state $I_0 \not\equiv 0$, the solution (S, I) of Eq* (2.1) *satisfies*

$$\liminf_{t\to\infty} \left(\inf_{x\in\overline{\Omega}} I(x,t) \right) \ge \eta.$$

Theorem 3. *Under the assumption that $\mathcal{R}_0 > 1$, the infection-free steady state becomes a repeller, and System* (2.1) *admits uniform persistence as characterized in Definition 2.*

Proof. Define the following phase space:

$$X = C(\bar{\Omega}, \mathbb{R}^2_+), \quad X_0 = \{(S,I) \in X : I \not\equiv 0\}, \quad \partial X_0 = \{(S,I) \in X : I \equiv 0\}.$$

Let Φ_t denote the solution semiflow generated by System (2.1). By Theorem 2.3 and the uniform bound in Lemma 2.2, Φ_t is eventually bounded and point dissipative on X. Standard parabolic regularity implies that Φ_t is compact for every $t > 0$.

On ∂X_0, we have $I \equiv 0$, so S satisfies the scalar Robin–logistic problem

$$\partial_t S = d_S \Delta S + S(\rho(x) - \mu(x)S), \quad \frac{\partial S}{\partial \nu} + aS = 0.$$

By Proposition 2.4, the unique positive steady state $\hat{S}_a$ exists and is globally asymptotically stable for this scalar equation whenever $\lambda_S(a) > 0$. Sence, the only compact invariant set in ∂X_0 that is relevant to the global dynamics is $(\hat{S}_a, 0)$.

For contradiction, suppose that there exists a solution $(S(\cdot,t), I(\cdot,t)) \in X_0$ with

$$\|(S(\cdot,t), I(\cdot,t)) - (\hat{S}_a, 0)\|_{C(\bar{\Omega})} \to 0 \quad \text{as } t \to \infty.$$

Fix $\varepsilon > 0$ sufficiently small. Then for all large t, we then have $\|S(\cdot,t) - \hat{S}_a\|_{C(\bar{\Omega})} < \varepsilon$ and $\|I(\cdot,t)\|_{C(\bar{\Omega})} < \varepsilon$, so

$$\frac{S}{S+I} \;\geq\; 1-\varepsilon.$$

Consequently, the I-equation satisfies the following:

$$\partial_t I \;\geq\; d_I \Delta I + (\beta(x)(1-\varepsilon) - \gamma(x))I, \quad \frac{\partial I}{\partial \nu} + bI = 0.$$

Let λ_1^ε be the principal eigenvalue of the operator $d_I\Delta + \beta(x)(1-\varepsilon) - \gamma(x)$ under the Robin boundary condition. Since $\mathcal{R}_0 > 1$ implies $\lambda_1 > 0$, and the principal eigenvalue continuously depends on the coefficients, we may choose ε small enough so that $\lambda_1^\varepsilon > 0$. Let $\varphi_1^\varepsilon > 0$ be the corresponding principal eigenfunction. Setting $w(x,t) = \delta e^{\lambda_1^\varepsilon t}\varphi_1^\varepsilon(x)$ for $\delta > 0$ chosen so that $w(\cdot,0) \leq I(\cdot,T_0)$ at some time T_0, the parabolic comparison principle gives

$$I(x,t) \;\geq\; \delta e^{\lambda_1^\varepsilon t}\varphi_1^\varepsilon(x) \;\to\; +\infty \quad \text{as } t \to \infty,$$

contradicting the uniform boundedness of I. Hence, E_0 is a weak repeller for X_0.

The set $\{(\hat{S}_a, 0)\}$ is the only compact invariant set in $\omega(\partial X_0)$, and it is both isolated in X and acyclic (it admits no cyclic chain in ∂X_0). By the uniform persistence theorem for compact dissipative semiflows (see Magal and Zhao [34] and Zhao [35]), there exists $\eta > 0$ such that

$$\liminf_{t\to\infty} \inf_{x\in\bar{\Omega}} I(x,t) \;\geq\; \eta$$

for every solution with $I_0 \not\equiv 0$.

Theorem 4. *Let $\mathcal{R}_0 > 1$. System (2.1) has at least one strictly positive steady state $(\tilde{S}, \tilde{I})$ in the domain $\overline{\Omega}$. Furthermore, there exists a uniform gap between any such endemic steady state and the infection-free steady state $(\hat{S}, 0)$.*

Proof. By Theorem 4.2, the semiflow Φ_t is uniformly persistent on X_0. Together with the point dissipativity and compactness established in Section 2, the uniform persistence theorem guarantees the existence of a compact global attractor $\mathcal{A}$ for Φ_t in X_0, which is bounded away from ∂X_0; in particular,

$$\inf_{(S,I)\in\mathcal{A}} \inf_{x\in\bar{\Omega}} I(x) \geq \eta > 0.$$

Moreover, we may choose a bounded closed convex set $B \subset X_0$, bounded away from ∂X_0, such that $\Phi_t(B) \subset B$, $t \geq 0$, and $\inf_{(S,I)\in B} \inf_{x\in\bar{\Omega}} I(x) \geq \frac{\eta}{2} > 0$. For each $n \in \mathbb{N}$, the map $\Phi_{1/n} : B \to B$ is compact

and continuous. Hence, by the Schauder fixed-point theorem, there exists $U_n = (S_n, I_n) \in B$ such that $\Phi_{1/n}(U_n) = U_n$. Since $\Phi_{1/n}(U_n) = U_n$, the semigroup property implies

$$\Phi_1(U_n) = (\Phi_{1/n})^n(U_n) = U_n.$$

Thus, $\{U_n\} \subset \Phi_1(B)$. Since Φ_1 is compact and B is bounded, the sequence $\{U_n\}$ is precompact in X. Passing to a subsequence if necessary, we may assume that $U_n \to U_* = (\tilde{S}, \tilde{I}) \in B$. Now, We show that U_* is fixed under the whole semiflow. For any fixed $t \geq 0$, choose integers $k_n \geq 0$ such that $k_n/n \to t$. Since $\Phi_{1/n}(U_n) = U_n$, the semigroup property gives the following:

$$\Phi_{k_n/n}(U_n) = (\Phi_{1/n})^{k_n}(U_n) = U_n.$$

Letting $n \to \infty$ and using the continuity of Φ_t with respect to both t and the initial value, we obtain $\Phi_t(U_*) = U_*,\ t \geq 0$. Therefore, $U_* = (\tilde{S}, \tilde{I})$ is fixed under the whole semiflow. Since System (2.1) is autonomous, U_* is a genuine steady state of Eq (2.1), rather than merely a periodic orbit.

It remains to verify strict positivity. Since $U_* \in B \subset X_0$ and B is bounded away from ∂X_0, we have $\inf_{x\in\bar{\Omega}} \tilde{I}(x) \geq \frac{\eta}{2} > 0$. In particular, $\tilde{I} \not\equiv 0$. The steady-state equation for $\tilde{I}$ reads

$$d_I \Delta \tilde{I} + \left(\beta(x)\frac{\tilde{S}}{\tilde{S}+\tilde{I}} - \gamma(x)\right)\tilde{I} = 0, \quad x \in \Omega,$$

with

$$\frac{\partial \tilde{I}}{\partial \nu} + b\tilde{I} = 0, \quad x \in \partial\Omega.$$

Since the coefficient $\beta(x)\frac{\tilde{S}}{\tilde{S}+\tilde{I}} - \gamma(x)$ is bounded, the strong maximum principle together with Hopf's boundary lemma implies $\tilde{I}(x) > 0,\ x \in \bar{\Omega}$. An analogous argument applied to the $\tilde{S}$-equation gives $\tilde{S}(x) > 0,\ x \in \bar{\Omega}$.

Finally, let (S^*, I^*) be any endemic steady state of System (2.1). Since it generates a constant trajectory in X_0, the uniform persistence result in Theorem 4.2 gives

$$\inf_{x\in\bar{\Omega}} I^*(x) \geq \eta_0 > 0$$

for some constant η_0 independent of the particular endemic steady state. Hence, all endemic steady states are uniformly separated from the disease-free equilibrium $(\hat{S}_a, 0)$. The proof is complete.

5. Influence of boundary outflow on disease dynamics

Next, we explore how the outflow rate b shapes the asymptotic steady states of the solutions for Eq (2.1).

Theorem 5. *Suppose that $d_I > 0$, $b > 0$, and $\hat{\lambda} > 0 > \lambda^D(d_I)$, and assume the average growth rate is non-negative, (i.e., $\int_\Omega \beta(x)\,dx \geq \int_\Omega \gamma(x)\,dx$). Let $b_1(d_I)$ denote the unique critical threshold established in Proposition 3.2. Then, the following dynamical scenarios occur:*

(i) If the outflow rate satisfies $b > b_1$, the infection-free state $(\hat{S}, 0)$ acts as a global attractor for the system. In this case, every solution $(S, I) \in [C(\overline{\Omega})]^2$ with non-zero and positive initial data satisfies the following:

$$(S(\cdot, t), I(\cdot, t)) \xrightarrow{t\to\infty} (\hat{S}, 0).$$

(ii) When $0 < b < b_1$, the epidemic persists in a uniform sense, meaning that the infectious component is uniformly sustained above a fixed level $\eta > 0$. Specifically, for any initial condition $I_0 \not\equiv 0$, the infectious population remains bounded away from zero as follows:

$$\liminf_{t\to\infty}\left(\inf_{x\in\Omega} I(x,t)\right) \geq \eta. \tag{5.1}$$

In what follows, we focus on the one-dimensional setting $\Omega = (0, L)$. Within this framework, the diffusion rate d_I and the boundary outflow b are constants, while the epidemiological parameters are assumed to be spatially uniform as follows:

$$\beta(x) \equiv \beta > 0, \quad \gamma(x) \equiv \gamma > 0.$$

Under these assumptions, we denote the principal eigenvalue of the linearized problem derived from the I-equation by $\lambda^D(d_I)$, subject to zero Dirichlet data. This eigenvalue is explicitly given by

$$\lambda^D(d_I) = \beta - \gamma - \frac{d_I\pi^2}{L^2},$$

while the corresponding eigenvalue under homogeneous Neumann boundary conditions is given by

$$\widehat{\lambda} = \beta - \gamma.$$

Now, We distinguish three cases.

Case 1: $\widehat{\lambda} < 0$. In this case, $\beta < \gamma$, hence, the infection decays even without population outflow at the boundary. As a consequence, $\mathcal{R}_0(d_I, b) < 1$ holds for any $b > 0$, thus suggesting that the eradication of the disease is independent of the boundary outflow intervention.

Case 2: $\lambda^D(d_I) > 0$. This condition is equivalent to

$$\beta - \gamma > \frac{d_I\pi^2}{L^2},$$

and corresponds to a situation in which transmission is sufficiently strong relative to recovery. In this case, Proposition 3.3 (5)(a) implies that $\mathcal{R}_0(d_I, b) > 1$ for all $b > 0$, thereby showing that boundary outflow alone is insufficient to prevent the persistence of the disease. This suggests that if the disease's internal growth is potent enough to overcome even the maximum possible diffusion loss (the Dirichlet limit), then boundary-based control strategies lose their regulatory power.

Case 3: $\widehat{\lambda} > 0$ and $\lambda^D(d_I) < 0$. This is the only condition in which the boundary outflow b has a genuine impact on the disease dynamics. According to Proposition 3.2 (2)(b), the principal eigenvalue $\lambda_1(d_I, b_1)$ vanishes for a unique positive threshold b_1. Moreover, b_1 is characterized as the solution of

$$d_I\phi_1''(x) + (\beta - \gamma)\phi_1(x) = 0, \quad \text{for } x \in (0, L) \tag{5.2}$$

with symmetric Robin-type constraints

$$\phi_1'(0) - b_1\phi_1(0) = 0 \text{ and } \phi_1'(L) + b_1\phi_1(L) = 0. \tag{5.3}$$

where ϕ_1 is the associated positive eigenfunction. Therefore, the value b_1 separates two distinct dynamical regimes: The disease persists when $0 < b < b_1$ and becomes extinct for $b > b_1$. We directly characterize the threshold value b_1 under the above setting.

Theorem 6. *Under the one–dimensional homogeneous setting described above, assume that*

$$0 < \beta - \gamma < \frac{d_I \pi^2}{L^2};$$

then, the threshold $b_1 > 0$ given in Proposition 4 is explicitly represented by

$$b_1 = \sqrt{\frac{\beta-\gamma}{d_I}} \tan\left(\frac{L}{2}\sqrt{\frac{\beta-\gamma}{d_I}}\right) \tag{5.4}$$

proposition 6. *Under the assumptions of Theorem 6, the critical boundary outflow rate b_1 exhibits the following parameter dependence:*

- *b_1 decreases as either the diffusion rate d_I or the recovery rate γ increases;*
- *b_1 increases with respect to the transmission rate β and the domain size L.*

Proof. For convenience, we introduce the quantity

$$q = \sqrt{\frac{\beta-\gamma}{d_I}}, \quad qL \in (0, \pi),$$

under which the explicit formula (5.4) can be simplified as

$$b_1(q, L) = q \tan\left(\frac{qL}{2}\right). \tag{5.5}$$

A direct differentiation of b_1 with respect to q yields the following

$$\frac{\partial b_1}{\partial q} = \tan\left(\frac{qL}{2}\right) + \frac{qL}{2}\sec^2\left(\frac{qL}{2}\right).$$

Since $qL/2 \in (0, \pi/2)$, both $\tan(qL/2)$ and $\sec^2(qL/2)$ are strictly positive; hence, $\frac{\partial b_1}{\partial q} > 0$. Then the dependence of b_1 on d_I, γ, and β directly follows from the following partial derivatives of q:

$$\frac{\partial q}{\partial d_I} = -\frac{1}{2d_I}\sqrt{\frac{\beta-\gamma}{d_I}} < 0, \quad \frac{\partial q}{\partial \gamma} = -\frac{1}{2d_I q} < 0, \quad \frac{\partial q}{\partial \beta} = \frac{1}{2d_I q} > 0.$$

By the chain rule, $\frac{\partial b_1}{\partial d_I} < 0$, $\frac{\partial b_1}{\partial \gamma} < 0$, and $\frac{\partial b_1}{\partial \beta} > 0$. Moreover, differentiating Eq (5.5) with respect to L gives

$$\frac{\partial b_1}{\partial L} = \frac{q^2}{2}\sec^2\left(\frac{qL}{2}\right) > 0,$$

which completes the proof.

To complement the analytical results, we provide numerical illustrations of the threshold relation $b = b_1$ in Figures 2 and 3. The solid curve in each figure represents the critical threshold $b = b_1$. The yellow-shaded region above the curve corresponds to disease extinction, namely $b > b_1$, whereas the unshaded region below the curve corresponds to disease persistence, namely $0 < b < b_1$.

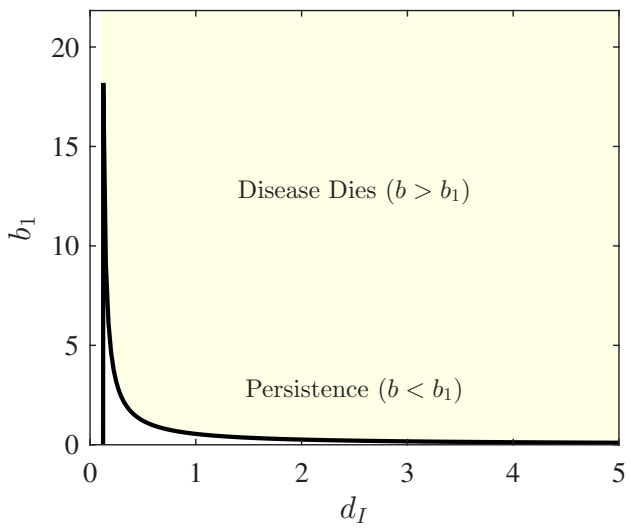

(a) Effect of the diffusion coefficient d_I.

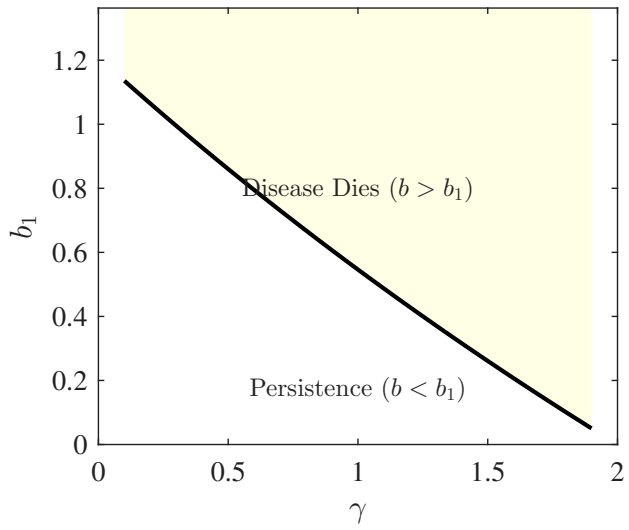

(b) Effect of the recovery rate γ.

Figure 2. Critical threshold b_1 versus (a) d_I and (b) γ. Fixed parameters: (a) $\gamma = 1, \beta = 2$, $L = 1$; (b) $d_I = 1, \beta = 2, L = 1$.

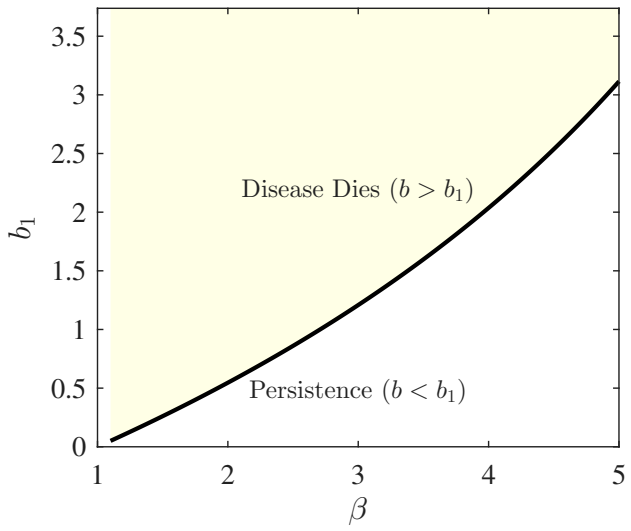

(a) Effect of the transmission rate β.

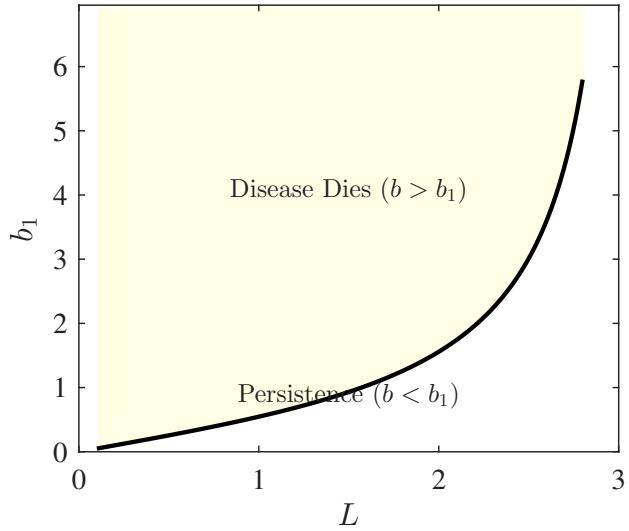

(b) Effect of the domain length L.

Figure 3. Critical threshold b_1 versus (a) β and (b) L. Fixed parameters: (a) $d_I = 1, \gamma = 1$, $L = 1$; (b) $d_I = 1, \gamma = 1, \beta = 2$.

To further validate the predicted threshold transition, we simulate the full system near the critical value. Taking $\beta = 1.6$, $\gamma = 1$, $d_I = 1$, and $L = 2$, Theorem 6 gives the following:

$$b_1 = \sqrt{\frac{\beta-\gamma}{d_I}} \tan\left(\frac{L}{2}\sqrt{\frac{\beta-\gamma}{d_I}}\right) \approx 0.758.$$

Then we choose three representative values $b = 0.70 < b_1$, $b \approx b_1$, $b = 0.85 > b_1$. Let

$$M_I(t) = \int_0^L I(x,t)\,dx$$

denote the total infected mass. At the final computational time, the corresponding values are approximately

$$M_I(T) = 6.35 \times 10^{-3}, \quad 9.24 \times 10^{-4}, \quad 1.78 \times 10^{-7},$$

respectively. These simulations are consistent with the theoretical prediction: the infected population persists when $b < b_1$, decays to zero when $b > b_1$, and exhibits slow transition behavior near the critical value.

More specifically, Figure 2(a) depicts how the threshold b_1 varies with the diffusion coefficient d_I. With β, γ, and L fixed, we see that b_1 decreases as d_I increases. This indicates that a faster diffusion of infected individuals reduces the level of boundary outflow required for disease elimination.

Figure 2(b) shows how b_1 varies with the recovery rate γ. With β, d_I, and L held constant, the threshold b_1 diminishes as γ increases. Hence, a higher recovery rate makes disease extinction achievable under a weaker boundary outflow.

Figure 3(a) illustrates the sensitivity of b_1 to the transmission rate β. Keeping d_I, γ, and L unchanged, b_1 increases with β, indicating that stronger disease transmission requires a larger outflow rate to suppress persistence.

Finally, Figure 3(b) presents the influence of the domain size L. For fixed d_I, β and γ, the threshold b_1 increases as the spatial domain becomes larger, thus reflecting that disease control through boundary outflow becomes more difficult in a larger habitat.

Taken together, these observations provide a clear quantitative interpretation of the role of population outflow in disease control under the logistic recruitment mechanism.

Numerical scheme and convergence verification

We briefly describe the numerical scheme used in the one-dimensional simulations. The spatial domain is taken as $\Omega = (0, L)$ and is divided into N uniform subintervals with mesh size $\Delta x = L/N$. Let $x_i = i\Delta x$ for $i = 0, 1, \ldots, N$. For a function u, the Robin boundary condition $\partial_\nu u + cu = 0$ is interpreted, on the interval $(0, L)$, as $u_x(0) = cu(0)$ and $u_x(L) = -cu(L)$. To preserve the second-order spatial accuracy near the boundary, we use second-order one-sided finite-difference formulas. More precisely,

$$\frac{-3u_0 + 4u_1 - u_2}{2\Delta x} = cu_0, \quad \frac{3u_N - 4u_{N-1} + u_{N-2}}{2\Delta x} = -cu_N.$$

Thus, the boundary values can be eliminated as follows:

$$u_0 = \frac{4u_1 - u_2}{3 + 2c\Delta x}, \quad u_N = \frac{4u_{N-1} - u_{N-2}}{3 + 2c\Delta x}.$$

Substituting these relations into the standard central difference formula for u_{xx} gives a second-order finite-difference approximation of the diffusion operator under Robin boundary conditions.

For the steady-state computation, the resulting nonlinear algebraic system is written as follows:

$$\begin{cases} d_S D_a S + F(S, I) = 0, \\ d_I D_b I + G(S, I) = 0, \end{cases}$$

where D_a and D_b denote the discrete Laplacian matrices incorporating the Robin boundary conditions with coefficients a and b, respectively, and

$$F(S, I) = S(\rho - \mu S) - \beta \frac{SI}{S + I} + \theta\gamma I, \quad G(S, I) = \beta \frac{SI}{S + I} - \gamma I.$$

The nonlinear algebraic system is solved by a damped Newton method until the steady-state residual is sufficiently small.

We perform a mesh-refinement test to verify the convergence of the spatial discretization. The solution computed on the finest mesh $N = 640$ is taken as the reference solution. We use the representative parameter values $L = 2$, $d_S = d_I = 1$, $\rho = \mu = 1$, $\theta = 0.8$, $\beta = 1.6$, $\gamma = 1$, $a = 1.2$, and $b = 0.50$. The convergence test is carried out with $b = 0.50$, which is away from the critical value and lies in the persistence region. The L^∞ errors of the steady-state profiles of S and I are reported in Table 1. The errors steadily decrease as the mesh is refined, and the observed orders are close to two for both components. This confirms the approximately second-order spatial accuracy of the finite-difference discretization.

Table 1. Mesh-refinement convergence test in the L^∞ norm. The reference solution is computed with $N = 640$. Parameters: $L = 2$, $d_S = d_I = 1$, $\rho = \mu = 1$, $\theta = 0.8$, $\beta = 1.6$, $\gamma = 1$, $a = 1.2$, and $b = 0.50$.

N	Δx	$\|E_S\|_{L^\infty}$	Order	$\|E_I\|_{L^\infty}$	Order
40	5.000×10^{-2}	4.919×10^{-4}	—	7.247×10^{-5}	—
80	2.500×10^{-2}	1.230×10^{-4}	2.00	1.813×10^{-5}	2.00
160	1.250×10^{-2}	2.945×10^{-5}	2.06	4.342×10^{-6}	2.06
320	6.250×10^{-3}	5.906×10^{-6}	2.32	8.709×10^{-7}	2.32

6. Conclusions

This study explored a spatially heterogeneous SIS reaction–diffusion framework that integrates logistic population regulation with boundary-mediated outflow. By introducing density-dependent growth, the model relaxes the population-conservation assumption and describes epidemic dynamics in open habitats subject to resource limitation and boundary movement. We rigorously demonstrated that the introduction of such non-linear regulation preserves the global existence and positivity of solutions while fundamentally shaping the long-term disease dynamics (Theorem 1).

The main contribution of this work is a threshold analysis for an SIS reaction–diffusion system that combines logistic growth and Robin boundary outflow. Since neither population conservation nor closed-boundary conditions hold, the existence of a positive disease-free equilibrium requires a Robin–logistic eigenvalue condition. Under this condition, $\mathcal{R}_0$ is shown to be a sharp threshold that

separates disease extinction from persistence. Additionaly, we also highlight the different roles of the two outflow rates: a shapes the disease-free susceptible profile, while b directly shifts the linearized infection threshold. Finally, an explicit critical value b_1 is derived in one spatial dimension, and its monotone dependence on d_I, β, γ, and L is established.

A central finding of our analysis is that the spectral parameter $\mathcal{R}_0$ acts as a threshold criterion. Despite the lack of population conservation, $\mathcal{R}_0$ remains the decisive predictor for disease outcome: the extinction regime is globally attractive when $\mathcal{R}_0 < 1$, whereas the disease persists uniformly if $\mathcal{R}_0 > 1$(Theorems 3 and 4). Our results reveal that while logistic growth complicates the global attractor's structure, it does not shift the critical bifurcation point defined by $\mathcal{R}_0$ at the infection-free state. These results confirm that the threshold principle remains the definitive threshold criterion in the study of open epidemic systems with complex demographic structures.

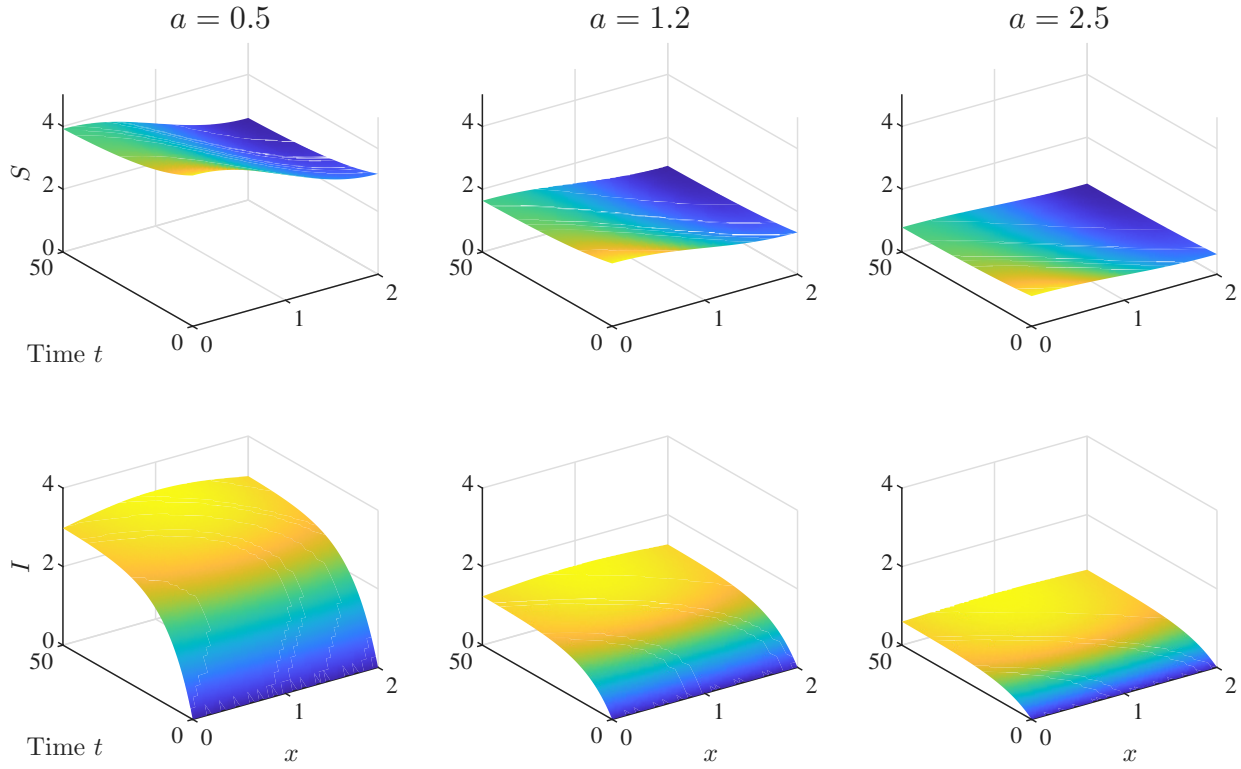

Figure 4. Time evolution of the solution of (2.1) for different values of a. Top row: $S(x,t)$. Bottom row: $I(x,t)$. Parameters: $\Omega = (0,2)$, $\beta = 1.6$, $b = 0.8$, and $d_S = d_I = \rho = \mu = \gamma = \theta = 1$. The columns from left to right correspond to $a = 0.5$, 1.2, and 2.5, respectively.

Our investigation highlights a critical asymmetry between the roles of susceptible and infected outflow. While the outflow rate of susceptible individuals alters the spatial distribution and equilibrium sizes, it leaves the threshold $\mathcal{R}_0$ invariant (Figure 4). Conversely, the removal of infected individuals acts as a powerful control mechanism (Figure 5). We identified a critical threshold b_1 that separates extinction from persistence, thus indicating that intensifying boundary leakage can effectively eradicate the disease (Theorem 5). From a public health perspective, this suggests that interventions which target the containment or selective removal of the infectious cohort at the boundary are far more efficient than generalized population movement controls. In the one-dimensional case, we further elucidated

how b_1 monotonically depends on vital factors such as the transmission intensity, recovery rate, and habitat size (Figures 2 and 3). These analytical sensitivities provide a theoretical basis to predict how changes in environmental connectivity or pathogen virulence might shift the required intensity of boundary-mediated control.

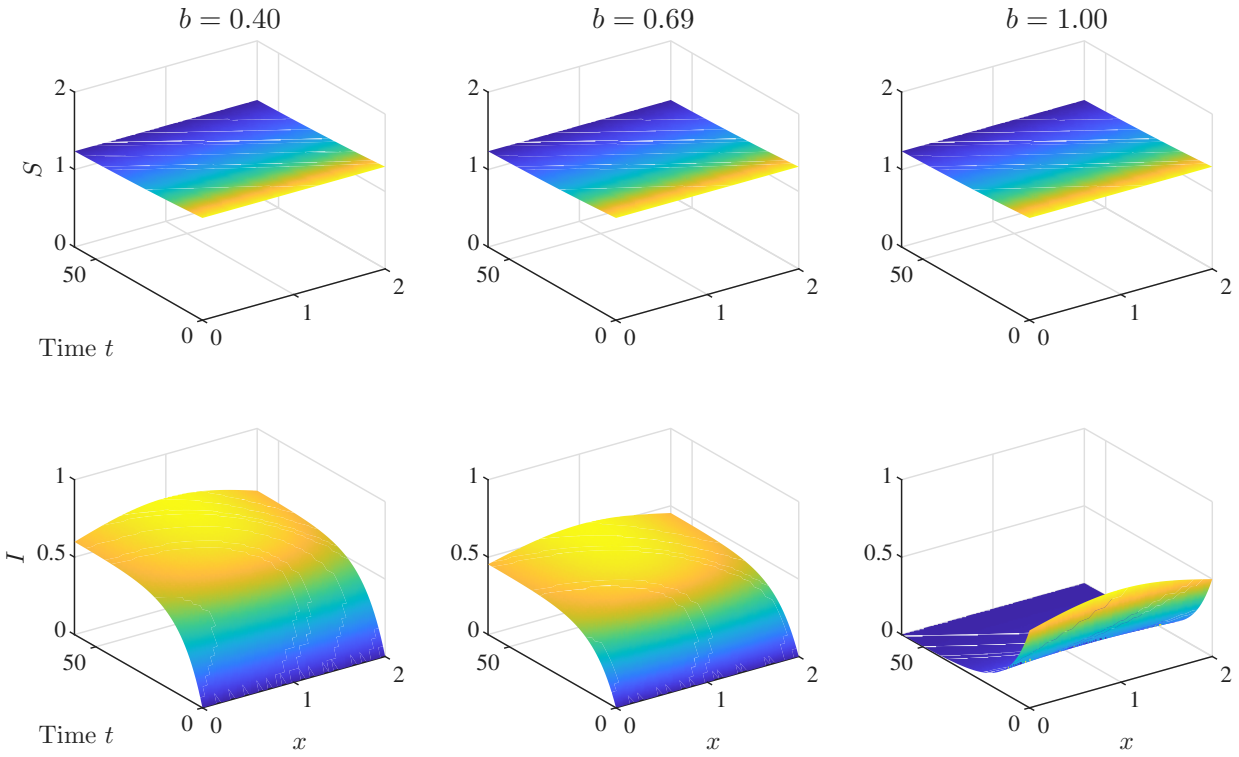

Figure 5. Time evolution of the solution of (2.1) for different values of b. Top row: $S(x,t)$. Bottom row: $I(x,t)$. Simulation settings: $\Omega = (0,2), \beta = 1.6, a = 1$, and $d_S = d_I{=}\rho = \mu{=}\theta = 1$. The outflow b is varied as 0.40 (left), 0.69 (middle), and 1.00 (right), positioned relative to the critical threshold $b_1 \approx 0.76$.

Biologically, these results suggest that boundary-mediated interventions can be as effective as internal controls, even in the presence of natural population regulation. Mathematically, this work provides a tractable paradigm to analyze non-conserved populations in spatial models. Future extensions may incorporate more intricate demographic features, such as state-dependent boundary conditions or multi-patch connectivity, to further explore the interplay between environmental non-homogeneity and density-dependent regulation of infectious diseases. The latter direction would require different tools for fractional derivatives and memory-dependent dynamics, and is left for future study.

Use of AI tools declaration

The authors declare that no generative-AI tools were used to generate the scientific content, mathematical analysis, numerical results, figures, or conclusions of this study. AI-assisted language tools were used only for minor English polishing. The authors reviewed and verified the final manuscript and take full responsibility for its content.

Acknowledgments

The authors would like to thank the editor and the anonymous reviewers for their valuable comments and constructive suggestions, which helped improve the quality and clarity of this manuscript.

Conflict of interest

Feng Li is a guest editor for *Networks and Heterogeneous Media*, and was not involved in the editorial review or the decision to publish this article. All authors declare that they have no competing interests.

Author contributions

The author: Pan Yifei, is the contributor to conceptualization, methodology, formal analysis, numerical simulation, writing–original draft, writing–review and editing. The author: Heejung Byun, is the contributor to supervision, methodology and validation. The author: Li Feng, is the contributor to ethodology, formal analysis and validation. All authors have read and approved the final manuscript.

Declaration

Data will be made available on reasonable request.

References

1. L. J. S. Allen, B. M. Bolker, Y. Lou, A. L. Nevai, Asymptotic profiles of the steady states for an SIS epidemic reaction–diffusion model, *Discrete Contin. Dyn. Syst.*, **21** (2008), 1–20. https://doi.org/10.3934/dcds.2008.21.1
2. Y. Lou, X. Q. Zhao, A reaction–diffusion malaria model with incubation period in the vector population, *J. Math. Biol.*, **62** (2011), 543–568. https://doi.org/10.1007/s00285-010-0346-8
3. Z. G. Bai, Y. Lou, Periodic environments and persistence of diffusive epidemic models, *J. Differ. Equations*, **266** (2019), 7658–7699. https://doi.org/10.1016/j.jde.2018.12.008
4. R. Peng, X. Q. Zhao, A reaction–diffusion SIS epidemic model in a time-periodic environment, *Nonlinearity*, **25** (2012), 1451–1471. https://doi.org/10.1088/0951-7715/25/5/1451
5. J. Li, X. Zou, Modeling spatial spread of infectious diseases with a fixed latent period in a spatially continuous domain, *Bull. Math. Biol.*, **71** (2009), 2048–2079. https://doi.org/10.1007/s11538-009-9457-z
6. Y. Li, W. T. Li, G. Lin, Traveling waves of a delayed diffusive SIR epidemic model, *Commun. Pure Appl. Anal.*, **14** (2015), 1001–1022. https://doi.org/10.3934/cpaa.2015.14.1001
7. Y. Lou, W. M. Ni, Diffusion, advection and environment heterogeneity in ecological and epidemic models, *J. Differ. Equations*, **244** (2008), 117–143. https://doi.org/10.1016/j.jde.2007.08.024
8. S. S. Chen, J. P. Shi, Z. S. Shuai, Y. X. Wu, Asymptotic profiles of the steady states for an SIS epidemic patch model with asymmetric connectivity matrix, *J. Math. Biol.*, **80** (2020), 2327–2361. https://doi.org/10.1007/s00285-020-01497-8

9. H. C. Li, R. Peng, Dynamics and asymptotic profiles of endemic equilibrium for SIS epidemic patch models, *J. Math. Biol.*, **79** (2019), 1279–1317. https://doi.org/10.1007/s00285-019-01395-8
10. R. H. Cui, H. C. Li, R. Peng, M. L. Zhou, Concentration behavior of endemic equilibrium for a reaction–diffusion–advection SIS epidemic model with mass action infection mechanism, *Calc. Var. Partial Differ. Equations*, **60** (2021), 184. https://doi.org/10.1007/s00526-021-01992-w
11. Y. Lou, R. B. Salako, Mathematical analysis of the dynamics of some reaction–diffusion models for infectious diseases, *J. Differ. Equations*, **370** (2023), 424–469. https://doi.org/10.1016/j.jde.2023.06.018
12. R. Peng, Asymptotic profiles of the positive steady state for an SIS epidemic reaction–diffusion model. Part I, *J. Differ. Equations*, **247** (2009), 1096–1119. https://doi.org/10.1016/j.jde.2009.05.002
13. R. Peng, S. Q. Liu, Global stability of the steady states of an SIS epidemic reaction–diffusion model, *Nonlinear Anal.*, **71** (2009), 239–247. https://doi.org/10.1016/j.na.2008.10.043
14. R. Peng, F. Q. Yi, Asymptotic profile of the positive steady state for an SIS epidemic reaction–diffusion model: Effects of epidemic risk and population movement, *Physica D*, **259** (2013), 8–25. https://doi.org/10.1016/j.physd.2013.05.006
15. B. Li, H. C. Li, Y. C. Tong, Analysis on a diffusive SIS epidemic model with logistic source, *Z. Angew. Math. Phys.*, **68** (2017), 96. https://doi.org/10.1007/s00033-017-0845-1
16. K. Deng, Asymptotic behavior of an SIR reaction–diffusion model with a linear source, *Discrete Contin. Dyn. Syst. Ser. B*, **24** (2019), 5945–5957. https://doi.org/10.3934/dcdsb.2019114
17. B. Li, Q. Y. Bie, Long-time dynamics of an SIRS reaction–diffusion epidemic model, *J. Math. Anal. Appl.*, **475** (2019), 1910–1926. https://doi.org/10.1016/j.jmaa.2019.03.062
18. C. X. Lei, J. Xiong, X. H. Zhou, Qualitative analysis on an SIS epidemic reaction–diffusion model with mass action infection mechanism and spontaneous infection in a heterogeneous environment, *Discrete Contin. Dyn. Syst. Ser. B*, **25** (2020), 81–98. https://doi.org/10.3934/dcdsb.2019173
19. Z. L. Feng, H. R. Thieme, Recurrent outbreaks of childhood diseases revisited: The impact of isolation, *Math. Biosci.*, **128** (1995), 93–130. https://doi.org/10.1016/0025-5564(94)00069-C
20. J. M. Hyman, J. Li, Modeling the effectiveness of isolation strategies in preventing STD epidemics, *SIAM J. Appl. Math.*, **58** (1998), 912–925. https://doi.org/10.1137/S003613999630561X
21. Q. Pan, J. C. Huang, H. Wang, An SIRS model with nonmonotone incidence and saturated treatment in a changing environment, *J. Math. Biol.*, **85** (2022), 23. https://doi.org/10.1007/s00285-022-01787-3
22. W. D. Wang, S. G. Ruan, Bifurcations in an epidemic model with constant removal rate of the infectives, *J. Math. Anal. Appl.*, **291** (2004), 775–793. https://doi.org/10.1016/j.jmaa.2003.11.043
23. Y. Hu, Y. Jin, J. Wang, Dynamics of a reaction–diffusion SIS epidemic model with population outflow on the boundary, *J. Differ. Equations*, **437** (2025), 113396. https://doi.org/10.1016/j.jde.2025.113396
24. J. Wang, K. Wang, T. Zheng, P. Zhou, Z. Teng, Qualitative analysis on a reaction–diffusion SIS epidemic model with nonlinear incidence and Dirichlet boundary, *Chaos Solitons Fractals*, **182** (2024), 114744. https://doi.org/10.1016/j.chaos.2024.114744

25. Y. Hu, Y. Jin, J. Wang, Dynamics of a reaction–diffusion SIS epidemic model with a control zone, *SIAM J. Appl. Math.*, **84** (2024), 2569–2589. https://doi.org/10.1137/24M1652374

26. R. B. Salako, Y. Wu, On the dynamics of an epidemic patch model with mass-action transmission mechanism and asymmetric dispersal patterns, *Stud. Appl. Math.*, **152** (2024), 1208–1250. https://doi.org/10.1111/sapm.12674

27. C. V. Pao, *Nonlinear Parabolic and Elliptic Equations*, Plenum Press, New York, 1992. https://doi.org/10.1007/978-1-4615-3034-3

28. H. C. Li, R. Peng, F. B. Wang, Varying total population enhances disease persistence: Qualitative analysis on a diffusive SIS epidemic model, *J. Differ. Equations*, **262** (2017), 885–913. https://doi.org/10.1016/j.jde.2016.09.044

29. D. Gilbarg, N. S. Trudinger, *Elliptic Partial Differential Equations of Second Order*, Classics in Mathematics, Springer, Berlin, 2001. https://doi.org/10.1007/978-3-642-61798-0

30. L. C. Evans, *Partial Differential Equations*, 2nd edition, American Mathematical Society, Providence, 2010. Available from: https://bookstore.ams.org/gsm-19-r.

31. R. S. Cantrell, C. Cosner, *Spatial Ecology via Reaction–Diffusion Equations*, John Wiley & Sons Ltd., Chichester, 2003. https://doi.org/10.1002/0470871296

32. R. Peng, G. H. Zhang, M. L. Zhou, Asymptotic behavior of the principal eigenvalue of a linear second order elliptic operator with small/large diffusion coefficient, *SIAM J. Math. Anal.*, **51** (2019), 4724–4753. https://doi.org/10.1137/18M1217577

33. W. D. Wang, X. Q. Zhao, Basic reproduction numbers for reaction–diffusion epidemic models, *SIAM J. Appl. Dyn. Syst.*, **11** (2012), 1652–1673. https://doi.org/10.1137/120872942

34. P. Magal, X. Q. Zhao, Global attractors and steady states for uniformly persistent dynamical systems, *SIAM J. Math. Anal.*, **37** (2005), 251–275. https://doi.org/10.1137/S0036141003439173

35. X. Q. Zhao, Uniform persistence and periodic coexistence states in infinite-dimensional periodic semiflows with applications, *Can. Appl. Math. Q.*, **3** (1995), 473–495. Available from: https://www.math.mun.ca/~zhao/Selectpapers/Zhao1995CAMQpub.pdf.

AIMS Press